3 1176 00116 0267

NATIONAL ADVISORY COMMITTEE FOR AERONAUTICS

TECHNICAL NOTE

No. 1175

FEB 14 1947

LIFTING-SURFACE-THEORY ASPECT-RATIO CORRECTIONS TO THE LIFT AND HINGE-MOMENT PARAMETERS FOR FULL-SPAN ELEVATORS ON HORIZONTAL TAIL SURFACES

By Robert S. Swanson and Stewart M. Crandall

Langley Memorial Aeronautical Laboratory
Langley Field, Va.

Washington
February, 1947

N A C A LIBRARY
LANGLEY MEMORIAL AERONAUTICAL
LABORATORY
Langley Field, Va.

NATIONAL ADVISORY COMMITTEE FOR AERONAUTICS

TECHNICAL NOTE NO. 1175

LIFTING-SURFACE-THEORY ASPECT-RATIO CORRECTIONS TO THE LIFT AND HINGE-MOMENT PARAMETERS FOR FULL-SPAN ELEVATORS ON HORIZONTAL TAIL SURFACES

By Robert S. Swanson and Stewart M. Crandall

SUMMARY

A limited number of lifting-surface-theory solutions for wings with chordwise loadings resulting from angle of attack, parabolic-arc camber, and flap deflection are now available. These solutions were studied with the purpose of determining methods of extrapolating the results in such a way that they could be used to determine lifting-surface-theory values of the aspect-ratio corrections to the lift and hinge-moment parameters for both angle-of-attack and flap-deflection-type loading that could be used to predict the characteristics of horizontal tail surfaces from section data with sufficient accuracy for engineering purposes. Such a method was devised for horizontal tail surfaces with full-span elevators. In spite of the fact that the theory involved is rather complex, the method is simple to apply, and may be applied without any knowledge of lifting-surface theory.

A comparison of experimental finite-span and section values and of the estimated values of the lift and hinge-moment parameters for three horizontal tail surfaces was made to provide an experimental verification of the method suggested.

INTRODUCTION

One of the problems for which lifting-line theory has proved inadequate (see reference 1) is that of estimating the hinge-moment parameters of finite-span control

surfaces from section data. In reference 1 for which experimental data were available for three cases, satisfactory additional aspect-ratio corrections to the hinge moments of ailerons caused by chordwise loading due to angle of attack could be determined by means of lifting-surface theory.

Since the publication of reference 1, considerably more section and finite-span (tail surfaces and ailerons) hinge-moment data have become available, and in all cases the slope of the hinge-moment curve against angle of attack (measured at small angles of attack) could be predicted with satisfactory accuracy from the section data by means of the lifting-surface-theory aspect-ratio corrections. Although the lifting-surface-theory aspect-ratio corrections were determined from a linear theory and thus apply only to the range of angles of attack near zero, they are extremely valuable for defining the stick-force gradient for the important high-speed case and are necessary for estimating the stick-free stability characteristics.

No lifting-surface-theory solutions were available, however, for wings with chordwise loading due to flap deflection. In order to obtain at least one such solution, an electromagnetic-analogy model (reference 2) of an elliptic wing of aspect ratio 3, with the chordwise loading corresponding to that of a 0.5-chord plain flap in two-dimensional flow, was constructed and tested (reference 3). In order to check the aspect-ratio corrections, determined from the results of the tests on the electromagnetic-analogy model, a semispan wing of the same plan form, same flap-chord ratio, and of the NACA 0009 airfoil section was constructed and tested in the Langley 4- by 6-foot vertical tunnel. The results of these tests are reported in reference 4.

As will be shown (see "Experimental Verification") the wind-tunnel tests provided a satisfactory check of the lifting-surface-theory aspect-ratio corrections both to the variation of hinge-moment coefficients with respect to angle of attack and to flap deflection.

Lifting-surface theory appeared to provide an accurate method of predicting finite-span characteristics from

section data. It might, however, be many years before sufficient lifting-surface-theory results will be available to determine the corrections for any plan form or flap-chord ratio because so many variables are involved. The lifting-surface-theory aspect-ratio corrections were determined for elliptic wings; however, they apparently could also be applied to unswept wings of other plan forms (see reference 1), even to the rectangular wing as indicated by the data of reference 5. That is, the hinge-moment slopes near zero angle of attack and zero flap deflection were predicted satisfactorily for the rectangular wing of aspect ratio 3 by use of theoretical results for the elliptic wing of aspect ratio 3.

The effect of the chord of the flap on the lifting-surface-theory aspect-ratio corrections was still to be determined; therefore, an electromagnetic-analogy model of an elliptic wing of aspect ratio 3 with elliptic chordwise as well as elliptic spanwise loading (approximately circular camber) (reference 3) and an elliptic wing of aspect ratio 6 simulating a steady roll were also tested (reference 6). A study of lifting-surface-theory results available (elliptic wings of aspect ratio 3 with angle-of-attack loading, 0.5-chord-flap loading, and parabolic-arc camber and an elliptic wing of aspect ratio 6 with angle-of-attack loading and steady-roll loading) was made and certain consistencies in the results were observed. From these observations the methods of extending the results so that they would provide lifting-surface-theory aspect-ratio corrections of satisfactory accuracy for engineering purposes were believed to be practical for horizontal tail surfaces of any flap-chord ratio, of aspect ratios from about 2 to 7, and with almost any plan form provided that the dihedral, taper, and sweep are not excessive. Insufficient lifting-surface-theory data are available, however, to predict the variation of hinge moments with elevator deflections for part-span elevators.

The actual method of determining lift and hinge-moment parameters from section data is presented herein in a fairly simple form in "Application of Method." The theoretical development of aspect-ratio corrections to lift and hinge-moment parameters for elliptic wings with constant-percentage-chord, full-span flaps and the methods used to extend these corrections to other plan forms are given in "Development of Method."

A comparison of the available experimental finite-span and section values and of the estimated values of lift and hinge-moment parameters is made for three horizontal tail surfaces and is presented in the section "Experimental Verification."

SYMBOLS

c_l	section lift coefficient $\left(\frac{\text{Section lift}}{qc}\right)$
C_L	tail lift coefficient $\left(\frac{\text{Lift}}{qS}\right)$
c_h	section hinge-moment coefficient $\left(\frac{\text{Section hinge moment}}{qc_e^2}\right)$
C_h	elevator hinge-moment coefficient $\left(\frac{\text{Hinge moment}}{q\bar{c}_e^2 b_e}\right)$
q	dynamic pressure $\left(\frac{1}{2}\rho V^2\right)$
ρ	mass density of air, slugs per cubic foot
α	angle of attack, degrees
α_o	angle of attack for two-dimensional flow, degrees
α_e	effective angle of attack, degrees
α_i	induced angle of attack, degrees
β	ratio of maximum ordinate of a thin parabolic-arc airfoil to its semichord $\left(\frac{z_{max}}{c/2}\right)$
β_i	induced parabolic-arc camber
z	ordinate of thin parabolic-arc airfoil
δ	elevator deflection, degrees
δ_t	tab deflection, degrees

A	aspect ratio (b^2/S)
λ	taper ratio $\left(\frac{\text{Tip chord}}{\text{Root chord}}\right)$
b	span of horizontal tail
b_e	span of elevator
c	chord of horizontal tail
c_s	chord of horizontal tail at center section
c_e	chord of elevator
$\bar{c}_e$	root-mean-square chord of elevator
x	chordwise distance from leading edge
y	spanwise distance from plane of symmetry
S	area
C_p	center-of-pressure coefficient, location of center of pressure as a function of the chord
$C_L/\Delta\alpha$	lift coefficient, resulting from a unit angle-of-attack deflection $\Delta\alpha$ over part of the tail span
M	Mach number
F	hinge-moment factor for theoretical load caused by streamline-curvature correction (reference 6)
B	internal balance factor (ratio of pressure difference across seal to pressure difference across vents)
η	experimentally determined reduction factor for F to include the effects of viscosity (reference 6)
K_L, K_H	functions to express variation of induced streamline curvature with flap-chord ratio
K, K_1, K_2	constants
E	Jones edge-velocity correction factor for lift

Δ increment

ϕ trailing-edge angle, degrees

w vertical component of induced velocity

w_w vertical component of induced velocity resulting from trailing vortices

V free-stream velocity

Γ_{max} circulation around tail center section

a_o section lift-curve slope

$$c_{l_\alpha} = \left(\frac{\partial c_l}{\partial \alpha_o}\right)_{\delta,\beta,\delta_t}$$

$$c_{l_\delta} = \left(\frac{\partial c_l}{\partial \delta}\right)_{\alpha_o,\beta,\delta_t}$$

$$c_{l_\beta} = \left(\frac{\partial c_l}{\partial \beta}\right)_{\alpha_o,\delta,\delta_t}$$

$$(\alpha_\delta)_{c_l} = \left|\left(\frac{\partial \alpha_o}{\partial \delta}\right)_{c_l}\right| = \frac{(\partial c_l/\partial \delta)_{\alpha_o,\beta,\delta_t}}{(\partial c_l/\partial \alpha)_{\delta,\beta,\delta_t}}$$

$$(\alpha_{\delta_t}) = \left|\left(\frac{\partial \alpha_o}{\partial \delta_t}\right)_{c_l}\right| = \frac{(\partial c_l/\partial \delta_t)_{\alpha_o,\beta,\delta_t}}{(\partial c_l/\partial \alpha)_{\delta,\beta,\delta_t}}$$

$$c_{h_\alpha} = \left(\frac{\partial c_h}{\partial \alpha_o}\right)_{\delta,\beta,\delta_t}$$

$$c_{h_\delta} = \left(\frac{\partial c_h}{\partial \delta}\right)_{\alpha_o,\beta,\delta_t}$$

$$c_{h_{\delta_t}} = \left(\frac{\partial c_h}{\partial \delta_t}\right)_{\alpha,\delta,\beta}$$

$$C_{L_\alpha} = \left(\frac{\partial C_L}{\partial \alpha}\right)_{\delta,\beta,\delta_t}$$

$$C_{L_\delta} = \left(\frac{\partial C_L}{\partial \delta}\right)_{\alpha,\beta,\delta_t}$$

$$C_{L_\beta} = \left(\frac{\partial C_L}{\partial \beta}\right)_{\alpha,\delta,\delta_t}$$

$$C_{h_\alpha} = \left(\frac{\partial C_h}{\partial \alpha}\right)_{\delta,\beta,\delta_t}$$

$$C_{h_\delta} = \left(\frac{\partial C_h}{\partial \delta}\right)_{\alpha,\beta,\delta_t}$$

$$\left(\alpha_\delta\right)_{C_L} = \left|\left(\frac{\partial \alpha}{\partial \delta}\right)_{C_L}\right| = \frac{\left(\partial C_L/\partial \delta\right)_{\alpha,\beta,\delta_t}}{\left(\partial C_L/\partial \alpha\right)_{\delta,\beta,\delta_t}}$$

$$C_{h_{\delta_t}} = \left(\frac{\partial C_h}{\partial \delta_t}\right)_{\alpha,\delta,\beta}$$

The subscripts outside the parenthesis indicate the factors held constant in determining the parameter.

Lifting-surface-theory parameters determined from lifting-surface-theory solutions of elliptic wings with two-dimensional chordwise loadings (these parameters are discussed when they appear in the report):

$\frac{\alpha_i}{c_l}$ induced angle of attack at the 0.5-chord line per unit section lift coefficient

$$\left(\frac{4\left(\frac{w_w b}{2\Gamma_{max}}\right)_{x/c=0.5}}{\pi A}\right)$$

$\frac{\Delta C_{L_{SC}}}{c_l}$ induced streamline-curvature lift coefficient per unit section lift coefficient

$$\left(\frac{8}{A\pi}\int_0^{1.0} \frac{\partial\left(\frac{wb}{2\Gamma_{max}}\right)}{\partial\left(\frac{x}{c}\right)}\left(\frac{c}{c_s}\right) d\left(\frac{y}{b/2}\right)\right)$$

$\frac{\Delta c_{h_{SC}}}{c_l}$ induced streamline-curvature hinge-moment coefficient per unit section lift coefficient

$$\left(\frac{F_\eta}{(c_e/c)^2}\frac{3}{A\pi}\int_0^{1.0}\frac{\partial\left(\frac{wb}{2\Gamma_{max}}\right)}{\partial\left(\frac{x}{c}\right)}\left(\frac{c}{c_s}\right)^2 d\left(\frac{y}{b/2}\right)\right)$$

Subscripts:

LL	lifting-line theory
LS	lifting-surface theory
av	average
max	maximum
f, δ	flap-type chordwise loading
b	balance
α	angle-of-attack-type chordwise loading
SC	streamline curvature
β	parabolic-arc camber chordwise loading
e	elevator or effective
t	tab
ell	elliptic
2	determined from two-dimensional loading condition

APPLICATION OF METHOD

GENERAL METHOD

The section lift parameters $\left(c_{l_\alpha},\ c_{l_\delta},\ \text{and consequently}\ (\alpha_\delta)_{c_l}\right)$ and section hinge-moment parameters $\left(c_{h_\alpha}\ \text{and}\ c_{h_\delta}\right)$ are assumed available for the airfoil

sections and flap arrangement of the horizontal tail at the Reynolds number, Mach number, and turbulence conditions of the finite-span-horizontal tail. The method accounts for first-order compressibility effects, provided that the section values of the lift and hinge-moment parameters are determined at the proper value of Mach number.

LIFT

The Parameter C_{L_α}

The slope of the curve of lift coefficient plotted against angle of attack at small angles of attack may be found from figure 1. The slope C_{L_α} is given as a function of the aspect ratio A and the slope of the section lift curve c_{l_α}.

Effectiveness parameter $(\alpha_\delta)_{C_L}$

The value of the finite-span effectiveness parameter $(\alpha_\delta)_{C_L}$ is found from the section values $(\alpha_\delta)_{c_l}$ in two steps (from figs. 2 and 3) if the horizontal tail does not have constant-percentage-chord elevators. The effectiveness of elevators that have a variable value of the section effectiveness parameter $(\alpha_\delta)_{c_l}$ is found by a mechanical integration of the parameter $\frac{C_L/\Delta\alpha}{(C_L/\Delta\alpha)_{max}}$ presented in figure 2 as indicated by the following formula:

$$(\alpha_\delta)_{C_{L_{LL}}} = \int_0^{1.0} (\alpha_\delta)_{c_l} \, d\left[\frac{C_L/\Delta\alpha}{(C_L/\Delta\alpha)_{max}}\right] \tag{1}$$

The values of $(\alpha_\delta)_{c_l}$ are plotted against the value of $\frac{C_L/\Delta\alpha}{(C_L/\Delta\alpha)_{max}}$ for all points $\frac{y}{b/2}$ along the elevator span. The area under the curve is equal to $(\alpha_\delta)_{C_{L_{LL}}}$.

If $(\alpha_\delta)_{c_l}$ has a constant value along the elevator span

$$(\alpha_\delta)_{C_{L_{LL}}} = (\alpha_\delta)_{c_l}$$

The corrected lifting-surface-theory value of $(\alpha_\delta)_{C_L}$ is estimated from figure 3. The procedure is to estimate the average value of c_e/c over the elevator span and determine the value of $\left[\frac{(\alpha_\delta)_{C_L}}{(\alpha_\delta)_{c_l}}\right]_{LS}$ from figure 3. This ratio is multiplied by the value of $(\alpha_\delta)_{C_{L_{LL}}}$ determined from the curves of figure 2 or by the section value $(\alpha_\delta)_{c_l}$ if $(\alpha_\delta)_{C_{L_{LL}}} = (\alpha_\delta)_{c_l}$.

The Parameter C_{L_δ}

The slope C_{L_δ} of the curve of lift coefficient plotted against elevator deflection for small values of elevator deflection is equal to the product of C_{L_α} and $(\alpha_\delta)_{C_L}$, which were found previously; that is,

$$C_{L_\delta} = C_{L_\alpha}(\alpha_\delta)_{C_L} \tag{2}$$

HINGE MOMENTS

The Parameter C_{h_α}

The slope C_{h_α} of the curve of hinge-moment coefficient plotted against angle of attack at small angles of attack may be found with satisfactory accuracy from the following equation:

$$C_{h_\alpha} = (c_{h_\alpha})_{av_\alpha}\left[1 - \left(\frac{\alpha_i}{\alpha}\right)_{LS}\right] + (\Delta C_{h_\alpha})_{SC} \tag{3}$$

In figure 4 are presented values of the parameter $\frac{(\alpha_i/\delta)_{LS}}{(\alpha_\delta)_{c_l}}$. The values of this parameter for $\frac{c_e}{c} = 1.0$ are equal to $(\alpha_i/\alpha)_{LS}$ since a tail surface at an angle of attack α may be considered a tail surface with a full-chord flap having a deflection δ.

Values of $(\Delta C_{h_\alpha})_{SC}$ are equal to values of $(\Delta C_{h_\delta})_{SC}$ and c_{l_δ} is equal to c_{l_α} when $\frac{c_e}{c} = 1.0$. These values may be found from figures 5, 6, and 7. In figure 5 are presented values of the parameter

$$(\Delta C_{h_\delta})_{SC} \frac{(c_e/c)^2}{F\eta c_{l_\delta}} A\left(A\sqrt{1 - M^2} + 4.21\right) \sqrt{1 - M^2}$$

as a function of $A\left(0.1/c_{l_\alpha}\right)$. Values of the aspect-ratio factor $\frac{1}{A\left(A\sqrt{1 - M^2} + 4.21\right) \sqrt{1 - M^2}}$ are given in figure 6 and values of $\frac{F}{(c_e/c)^2}$ for elevators with plain $(c_b = 0)$ and exposed-overhang balance c_b in figure 7(a). If an internally balanced elevator is used figure 7(b) and the estimated balance factor B, which is one minus the seal leakage ratio, should be used. The average value of c_e/c is used if this factor varies across the elevator span. The value $\eta = 1 - 0.0005\phi^2$.

If the values of c_{h_α} for the various sections across the span do not vary from the mean value more than about 10 percent and the taper ratio of the tail surface is about 0.5, it will usually be satisfactory to estimate $(c_{h_\alpha})_{av_\alpha}$ without making an actual spanwise integration. If the values of c_{h_α} vary more than about 10 percent, it will be necessary to make an integration to obtain answers which are sufficiently correct. The following integral is then used to evaluate $(c_{h_\alpha})_{av_\alpha}$

$$\left(c_{h_\alpha}\right)_{av_\alpha} = \frac{1}{\frac{b_e}{b}\bar{c}_e^{\,2}} \int_0^{b_e/b} \left(\frac{\alpha_e}{\alpha_{e_{ell}}}\right)_{LS} c_{h_\alpha} c_e^{\,2}\, d\left(\frac{y}{b/2}\right) \tag{4}$$

Values of $\left(\frac{\alpha_e}{\alpha_{e_{ell}}}\right)_{LS}$ are given in figure 8.

The Parameter C_{h_δ}

The slope C_{h_δ} of the curve of hinge-moment coefficient plotted against elevator deflection at small values of elevator deflection may be found with satisfactory accuracy from the following equation:

$$C_{h_\delta} = \left(c_{h_\delta}\right)_{av} - \left(\frac{\alpha_i}{\delta}\right)_{LS} \left(c_{h_\alpha}\right)_{av_\delta} + \left(\Delta C_{h_\delta}\right)_{SC} \tag{5}$$

where values of $\left(c_{h_\delta}\right)_{av}$ may be averaged by eye if c_{h_δ} varies only a small amount or by the following equation if it varies considerably

$$\left(c_{h_\delta}\right)_{av} = \frac{1}{\frac{b_e}{b}\bar{c}_e^{\,2}} \int_0^{b_e/b} c_{h_\delta} c_e^{\,2}\, d\left(\frac{y}{b/2}\right) \tag{6}$$

The induced-angle-of-attack parameter $\left(\alpha_i/\delta\right)_{LS}$ may be determined from figure 4 for the average value of c_e/c.

The following integral is used for the evaluation of $\left(c_{h_\alpha}\right)_{av_\delta}$

$$\left(c_{h_\alpha}\right)_{av_\delta} = \frac{1}{\frac{b_e}{b}\bar{c}_e^{\,2}} \int_0^{b_e/b} \left(\frac{\alpha_i}{\alpha_{i_{ell}}}\right)_{LL} c_{h_\alpha} c_e^{\,2}\, d\left(\frac{y}{b/2}\right) \tag{7}$$

Values of the parameter $\left(\alpha_i/\alpha_{i_{ell}}\right)_{LL}$ may be determined from figure 9. Values of the streamline-curvature correction $\left(\Delta C_{h_\delta}\right)_{SC}$ may be determined from figures 5, 6, and 7 by use of an average value of c_e/c over the elevator span.

The Parameter $C_{h_{\delta_t}}$

The aspect-ratio corrections for partial-span tabs are usually smaller than for full-span tabs. An analytical method of calculating the corrections is not available but, according to the data presented in reference 7, an average reduction factor of 0.90 is satisfactory; that is

$$C_{h_{\delta_t}} = \frac{0.90}{\frac{b_e}{b/2}\bar{c}_e^{\,2}} \int_{-\frac{b_e}{b}}^{\frac{b_e}{b}} c_{h_{\delta_t}} c_e^{\,2}\, d\left(\frac{y}{b/2}\right) \tag{8}$$

where the integration need be made only across the span of the tab.

For full-span tabs the aspect-ratio correction is a little larger and may be computed more accurately by use of the following approximation. The same reduction in the value of c_{h_δ} caused by aspect ratio (last two terms of equation (5)) may be assumed to apply to $c_{h_{\delta_t}}$ provided that it is multiplied by the ratio of the tab-lift effectiveness $\left(\alpha_{\delta_t}\right)_{c_l}$ to the elevator-lift effectiveness $\left(\alpha_\delta\right)_{c_l}$. Thus,

$$C_{h_{\delta_t}} = \left(c_{h_{\delta_t}}\right)_{av} + \frac{\left(\alpha_{\delta_t}\right)_{c_l}}{\left(\alpha_\delta\right)_{c_l}} \left[-\left(\frac{\alpha_i}{\delta}\right)_{LS} \left(c_{h_\alpha}\right)_{av_\delta} + \left(\Delta C_{h_\delta}\right)_{SC}\right] \tag{9}$$

where

$$-\left(\frac{\alpha_1}{\delta}\right)_{LS}\left(c_{h_\alpha}\right)_{av_\delta} + \left(\Delta C_{h_\delta}\right)_{SC}$$

was determined for the calculation of C_{h_δ} and

$$\left(c_{h_{\delta_t}}\right)_{av} = \frac{1}{\frac{b_e}{b/2}\,\bar{c}_e^{\,2}} \int_{-\frac{b_e}{b}}^{\frac{b_e}{b}} c_{h_{\delta_t}} c_e^{\,2}\, d\left(\frac{y}{b/2}\right) \tag{10}$$

DEVELOPMENT OF METHOD

AVAILABLE LIFTING-SURFACE-THEORY RESULTS

Analytic Solutions

A complete analytic solution of the elliptic wing has been obtained and presented in reference 8. The mathematical methods used were, however, extremely difficult and it does not seem to be practicable to obtain any numerical answers from this treatment except for the theoretical slope of the lift curve. The numerical values of the theoretical lift-curve slope of elliptic wings as given in reference 8 are presented in figure 10 (a section lift-curve slope of 2π per radian is used).

Robert T. Jones presented a theoretical correction, in reference 9, usually called the Jones edge-velocity correction, for the lift of elliptic wings at an angle of attack. The lift-curve slope obtained by applying the edge-velocity correction is given in figure 10. Jones has also obtained (unpublished) an edge-velocity correction for the damping-in-roll of elliptic wings.

Although the Jones edge-velocity correction gives only about two-thirds of the total theoretical correction to the slope of the lift curve (fig. 10) or to the damping-in-roll (reference 6), it has several very

practical uses because it is given by such an extremely simple formula. First, it may be used to calculate the downwash at the 0.5-chord points of the wing. Because the downwash at the 0.5-chord points gives the amount of lift load which has an angle-of-attack type of chordwise load distribution (references 6 and 10), this fact is especially valuable in estimating finite-span hinge-moment characteristics from section data. Secondly, the same formula that is used to apply the edge-velocity correction may be used as a reasonable basis of extrapolating other lifting-surface-theory results obtained for only one or two aspect ratios by use of the concept of an effective edge-velocity correction factor. (See reference 6.)

Some studies have been made of the possibility of using a finite number of "horseshoe" vortices to represent the actual continuous loading over the wing. Falkner has developed (reference 11) a procedure for laying out the horseshoe vortices and has selected what he considers to be the most representative points for computing the downwash for that layout of vortices for wings at an angle of attack or with continuous camber.

Studies with the electromagnetic-analogy method of making lifting-surface-theory calculations (described in reference 2) have indicated that the vortices used to represent the continuous loading must be layed out very carefully in order to obtain the correct downwash, especially for arrangements with spanwise or chordwise discontinuities. Also, Falkner has two layouts only slightly different near the tip but which give very different values of the downwash. Thus it is believed that the results of any method using a finite number of horseshoe vortices must be examined with care.

Falkner's layout appears to give fairly satisfactory accuracy for the calculation of the lift-curve slope for cases of rather smooth loading. This layout, however, would probably be unsatisfactory for use for wings with flaps or ailerons deflected; at least this case would require a different layout of the horseshoe vortices and, therefore, different tables for use in the calculations. Also, the calculation of hinge-moment aspect-ratio corrections is considerably more critical than the calculation of the lift-curve slope. Falkner's results for the lift-curve slope are also presented in figure 10.

Semigraphical Solutions

Reference 12 presents a semigraphical method of determining the downwash for any continuous distribution of vortices in a plane such as a lifting surface. Some of the results obtained by this method are summarized in figure 11.

Electromagnetic-Analogy Solutions

The electromagnetic-analogy method of solving lifting-surface-theory problems (reference 2) has been used to solve several cases (references 2, 3, 6, and unpublished). A summary of some of these results is given in figure 11.

METHODS OF EXTENDING RESULTS OF AVAILABLE LIFTING-SURFACE-THEORY SOLUTIONS

Extending the limited number of lifting-surface-theory solutions, previously described, to apply to other aspect ratios and chord loadings required additional assumptions that would permit the evaluation of the various lifting-surface-theory parameters necessary for the evaluation of aspect-ratio corrections for elliptic wings with constant-percentage-chord full-span flaps. These assumptions are believed to be satisfactory according to present knowledge; however, they will undoubtedly be modified to some extent as additional lifting-surface-theory results become available.

The induced downwash at the 0.5 chord line, determined by lifting-surface-theory methods for elliptic wings of aspect ratios 3 and 6 with angle-of-attack-type chordwise loading, agrees with the downwash of elliptic wings computed by the use of the Jones edge-velocity correction factor E (reference 9). The edge-velocity correction factor may be used to estimate the downwash at the 0.5 chord line of elliptic wings. The relation for an elliptic wing of aspect ratio A with angle-of-attack-type chordwise loading may be shown to be

$$\left(\frac{wb}{2\Gamma_{max}}\right)_{\alpha} = \frac{A}{8} + \frac{1}{4} + \frac{A(E - 1)}{8}$$

The first of the right-hand terms $A/8$ represents the downwash induced by the bound (lift) vorticity and the last two terms represent that induced by the trailing vortices.

The center-of-pressure coefficient C_p is assumed to be the most important parameter with regard to the effects of chordwise loading. The lifting-surface-theory solution of reference 3 for an elliptic wing with parabolic-arc-camber chordwise loading may be then regarded as a solution for a wing with a chordwise loading corresponding to that of a plain flap of vanishingly small chord in two-dimensional flow since both have the same center-of-pressure location.

Lifting-surface-theory measurements for elliptic wings of aspect ratio 3 with various chordwise loadings show that the downwash induced at the 0.5 chord line by the trailing vortices is a linear function of the center-of-pressure coefficient. (See fig. 11(b).) For an elliptic wing of aspect ratio A with a chordwise loading having a center-of-pressure coefficient C_p, the downwash at the 0.5 chord line induced by the trailing vortices is therefore assumed to be given by

$$\frac{w_w b}{2\Gamma_{max}} = \frac{1}{4} + \left[\frac{A(E - 1)}{8}\right](2 - 4C_p)$$

Since $\alpha_i = \frac{w_w}{V}$ and $c_l = \frac{\pi A \Gamma_{max}}{2Vb}$, the parameter $\frac{\alpha_i}{c_l}$ is then

$$\frac{\alpha_i}{c_l} = \frac{1}{A\pi}\left[1 + A(E - 1)(1 - 2C_p)\right] \tag{11}$$

Streamline-curvature corrections for lift and hinge moment have been developed in references 6 and 10. The corrections are obtained by summing, across the wing, the parameter $\frac{\partial\left(wb/2\Gamma_{max}\right)}{\partial(x/c)}$ (a measure of the parabolic-arc camber (reference 3)) times the chord ratio c/c_s for the lift correction or times the chord ratio squared $\left(c/c_s\right)^2$ for the hinge-moment correction.

These streamline-curvature functions are assumed to vary with aspect ratio in the following manner for any chordwise loading:

$$\int_0^{1.0} \frac{\partial\left(wb/2\Gamma_{max}\right)}{\partial(x/c)} \frac{c}{c_s} \, d\left(\frac{y}{b/2}\right) = \frac{K_L}{A + K_1}$$

$$\int_0^{1.0} \frac{\partial\left(wb/2\Gamma_{max}\right)}{\partial(x/c)} \left(\frac{c}{c_s}\right)^2 d\left(\frac{y}{b/2}\right) = \frac{K_H}{A + K_2}$$

where K_L and K_H are functions of the chord loading. Then

$$\frac{\Delta C_{L_{SC}}}{c_l} = \frac{8}{A\pi} \frac{K_L}{A + K_1} \tag{12}$$

and

$$\frac{\Delta C_{h_{SC}}}{c_l} = \frac{F\eta}{(c_e/c)^2} \frac{3}{A\pi} \frac{K_H}{A + K_2} \tag{13}$$

By use of the available lifting-surface-theory data, K_1 and K_2 were evaluated as 5.69 and 4.21, respectively.

Values of the functions K_L and K_H are plotted in figure 12 against elevator-chord ratio c_e/c.

As in reference 6, the concept of an effective edge-velocity correction was used to extend the lifting-surface-theory results for the slopes of the lift-curves C_{L_α} and C_{L_δ}. The formula used to evaluate E_e, which is used for calculating C_{L_α} in reference 6, is

$$E_e = 1.65(E - 1) + 1$$

Similarly, the effective edge-velocity correction E_{e_f} for elliptic wings with full-span constant-percentage-chord flaps is

$$E_{e_f} = K(E_e - 1) + 1 \tag{14}$$

where K is a function of only the flap-chord ratio.

FORMULAS USED TO CALCULATE ASPECT-RATIO CORRECTIONS

General Discussion

For the problem of predicting the characteristics of finite-span control surfaces, it is preferable to determine the lifting-surface-theory solution in the form of corrections to the simpler lifting-line theory rather than to make complete analytic potential-flow solutions such as were obtained in reference 8. The main effects of viscosity can then be included by basing the finite-span estimations upon experimentally determined section data; this method is especially necessary for hinge-moment estimations. Thus, the only lifting-surface solutions that may be used for aspect-ratio corrections for hinge-moment estimations are those solutions for which the shape of the surface required to support a given lift distribution was determined. Corrections to the given lift distribution may then be determined by calculating the incremental lift distribution given by a surface

equal to the difference between the assumed surface and the calculated surface required to support the original given lift distribution. The changes in hinge-moment resulting from this incremental lift distribution can then be determined.

Formulas for determining these corrections to the span load distributions and rolling- and hinge-moment characteristics have been developed in connection with jet-boundary-correction problems (reference 10). These formulas are based on the assumption that the difference between the two surfaces is equivalent, at each section, to an increment of angle of attack plus an increment of parabolic-arc camber. The data of references 2 and 3 show that such assumptions are justified since the chordwise distribution of downwash is approximately linear. These formulas are based on thin airfoil theory and thus do not consider the effects of viscosity, wing thickness, or compressibility.

Viscosity.- The complete additional aspect-ratio correction consists of two parts. The main part results from the streamline curvature or induced parabolic-arc camber and the other part results from an additional increment of induced angle of attack (the angle at the 0.5c point) not determined by lifting-line theory. The second part of the correction is normally small, 5 to 10 percent of the first part of the correction. Some experimental data indicate that the effects of viscosity and wing thickness are to reduce the theoretical streamline-curvature correction by about 10 percent for airfoils with small trailing-edge angles. Thus, essentially the same final answer is obtained whether the corrections are applied in two parts (as should be done, strictly speaking) or whether they are applied in one part but using the full theoretical value of the streamline-curvature correction. The added simplicity of using a single correction rather than applying it in two parts led to the use of the method of application of reference 1.

The use of the single correction worked very well for the ailerons of reference 1, which were ailerons with small trailing-edge angles. In the present report it is desired to determine the proper aspect-ratio corrections for tail surfaces with beveled trailing edges. For these cases, for which viscous effects may be much more pronounced, the reduction in the theoretical

streamline-curvature correction may be considerably more than 10 percent. Also it may be easily seen that when C_{h_α} is positive, the effects of the reduction in the streamline-curvature correction and the additional downwash at the 0.5c point are additive rather than compensating. Although at present there are insufficient data to determine accurately the magnitude of the reduction in the streamline-curvature correction for beveled ailerons, the simplification of applying aspect-ratio corrections in a single step does not appear allowable for beveled ailerons. The corrections will, therefore, be determined in two separate parts in order to keep them perfectly general; one, a streamline-curvature correction and the other, an angle-of-attack correction. An examination of the experimental data available at present indicates that more nearly accurate values of the hinge moment resulting from streamline curvature are obtained by multiplying the theoretical values by an empirical factor η which is very nearly equal to $1 - 0.0005\phi^2$, ϕ being the trailing-edge angle in degrees; however, this factor will doubtless be modified when further experimental data are available.

Compressibility.- The effects of compressibility upon the additional aspect-ratio corrections were not considered in reference 1. First-order compressibility effects can be accounted for by application of the Prandtl-Glauert rule to lifting-surface-theory results (reference 13). This method consists in determining the incompressible flow characteristics of an equivalent wing whose chords are increased by the ratio $1/\sqrt{1 - M^2}$ where M is the ratio of the free-stream velocity to the velocity of sound. Because approximate methods of extrapolating the estimated lift and hinge-moment parameters to wings of any aspect ratio will be determined, the only estimations necessary are those of the hinge-moment and damping parameters corresponding to an equivalent wing of which the aspect ratio is decreased by the ratio $\sqrt{1 - M^2}$. The estimated parameters for the equivalent wing are then increased by the ratio $1/\sqrt{1 - M^2}$.

In most cases the changes in the aspect ratio and in the lift and hinge-moment parameters obtained by applying the ratios of $\sqrt{1 - M^2}$ can be shown to be simply equivalent to the changes obtained by using a

value of the section slope of the lift curve at the proper Mach number. The compressibility corrections were applied in this fashion; that is, by assuming that the section slope of the lift curve was experimentally determined at the proper value of Mach number in all cases except the case of the aspect-ratio extrapolation factor for streamline-curvature load. (See figs. 5 and 6.)

General Lifting-Surface-Theory Formulas for the Determination of Aerodynamic Characteristics of Elliptic Wings from Section Data

In the present section general lifting-surface-theory formulas for determining the aerodynamic characteristics of elliptic wings from section data are developed. In the section entitled "Extension of Formulas to Other Aspect Ratios and Plan Forms" methods of extending these results to apply to wings other than elliptic and further details of the methods of extending the results to other aspect ratios are presented.

Slope of lift curve C_{L_δ}.- In order to support, in three-dimensional flow, the load which would exist on an elliptic wing with full-span flap of constant-percentage chord if the flow were two-dimensional the wing, in addition to the flap deflection, must be given an induced angle of attack α_i and an induced parabolic-arc camber β_i. The induced angle of attack α_i is constant across the span, but the induced camber is not. If it is assumed that a value of β_i weighted in proportion to the chord can be used with the slope C_{L_β} to give the camber lift,

$$c_{l_\delta} = C_{L_\delta} + \left(\frac{\alpha_i}{\delta}\right)_2 C_{L_\alpha} + \left(\frac{\beta_i}{\delta}\right)_2 C_{L_\beta}$$

In order to calculate the characteristics of finite-span wings from section data the induced angle of attack and the induced camber per unit flap deflection for the three-dimensional lifting-surface load must be known. The finite-span lift-curve slope C_{L_δ} is then

$$C_{L_\delta} = c_{l_\delta} - \left(\frac{\alpha_i}{\delta}\right)_{LS} c_{l_\alpha} - \left(\frac{\beta_i}{\delta}\right)_{LS} c_{l_\beta} \tag{15}$$

Because an average value of β_i is to be used with theoretical values of c_{l_β}, it is convenient to write the last term of equation (15) as $\left(\Delta C_{L_\delta}\right)_{SC}$. Equation (15) may then be written,

$$C_{L_\delta} = c_{l_\delta} - \left(\frac{\alpha_i}{\delta}\right)_{LS} c_{l_\alpha} - \left(\Delta C_{L_\delta}\right)_{SC} \tag{16}$$

The induced loads $\left(\alpha_i/\delta\right)_{LS} c_{l_\alpha}$ and $\left(\Delta C_{L_\delta}\right)_{SC}$ are considered as positive quantities and the negative signs account for the fact they actually are downward loads.

The induced angle of attack for the lifting-surface load is a function of the two-dimensional flap load δc_{l_δ}, the induced (negative) angle-of-attack load $\alpha_{i_{LS}} c_{l_\alpha}$, and the induced (negative) camber load $\beta_{i_{LS}} c_{l_\beta}$; that is,

$$\alpha_{i_{LS}} = f\left(\delta c_{l_\delta}, -\alpha_{i_{LS}} c_{l_\alpha}, -\beta_{i_{LS}} c_{l_\beta}\right)$$

The value of $\left(\alpha_i/\delta\right)_{LS}$ is then the derivative of the function f with respect to δ and

$$\left(\frac{\alpha_i}{\delta}\right)_{LS} = \frac{\partial \alpha_{i_{LS}}}{\partial\left(\delta c_{l_\delta}\right)} \frac{d\left(\delta c_{l_\delta}\right)}{d\delta} + \frac{\partial \alpha_{i_{LS}}}{\partial\left(-\alpha_{i_{LS}} c_{l_\alpha}\right)} \frac{d\left(-\alpha_{i_{LS}} c_{l_\alpha}\right)}{d\delta} + \frac{\partial \alpha_{i_{LS}}}{\partial\left(-\beta_{i_{LS}} c_{l_\beta}\right)} \frac{d\left(-\beta_{i_{LS}} c_{l_\beta}\right)}{d\delta}$$

where

$$\frac{\partial\left(\alpha_{i_{LS}}\right)}{\partial\left(\delta c_{l_\delta}\right)} = \left(\frac{\alpha_i}{c_l}\right)_f$$

$$\frac{d\left(\delta c_{l_\delta}\right)}{d\delta} = c_{l_\delta}$$

$$\frac{\partial\alpha_{i_{LS}}}{\partial\left(-\alpha_{i_{LS}} c_{l_\alpha}\right)} = -\left(\frac{\alpha_i}{c_l}\right)_\alpha$$

$$\frac{d\left(-\alpha_{i_{LS}} c_{l_\alpha}\right)}{d\delta} = \left|-c_{l_\alpha}\left(\frac{\alpha_i}{\delta}\right)_{LS}\right|$$

$$= c_{l_\alpha}\left(\frac{\alpha_i}{\delta}\right)_{LS}$$

$$\frac{\partial\alpha_{i_{LS}}}{\partial\left(-\beta_{i_{LS}} c_{l_\beta}\right)} = -\left(\frac{\alpha_i}{c_l}\right)_\beta$$

and

$$\frac{d\left(-\beta_{i_{LS}} c_{l_\beta}\right)}{d\delta} = \left(\Delta C_{L_\delta}\right)_{SC}$$

As mentioned previously, the induced loads are considered as positive quantities even though they are actually downward loads. Thus

$$\left(\frac{\alpha_i}{\delta}\right)_{LS} = c_{l_\delta}\left(\frac{\alpha_i}{c_l}\right)_f - \left(\frac{\alpha_i}{\delta}\right)_{LS} c_{l_\alpha}\left(\frac{\alpha_i}{c_l}\right)_\alpha - \left(\Delta C_{L_\delta}\right)_{SC}\left(\frac{\alpha_i}{c_l}\right)_\beta \tag{17}$$

Similarly, the induced camber lift is obtained as

$$\left(\Delta C_{L_\delta}\right)_{SC} = c_{l_\delta}\left(\frac{\Delta C_{L_{SC}}}{c_l}\right)_f - \left(\frac{\alpha_i}{\delta}\right)_{LS} c_{l_\alpha}\left(\frac{\Delta C_{L_{SC}}}{c_l}\right)_\alpha - \left(\Delta C_{L_\delta}\right)_{SC}\left(\frac{\Delta C_{L_{SC}}}{c_l}\right)_\beta \tag{18}$$

Solving equations (17) and (18) simultaneously for $\left(\alpha_i/\delta\right)_{LS}$ and $\left(\Delta C_{L_\delta}\right)_{SC}$ gives

$$\left(\frac{\alpha_i}{\delta}\right)_{LS} = \frac{\left\{\left(\frac{\alpha_i}{c_l}\right)_f\left[1 + \left(\frac{\Delta C_{L_{SC}}}{c_l}\right)_\beta\right] - \left(\frac{\alpha_i}{c_l}\right)_\beta\left(\frac{\Delta C_{L_{SC}}}{c_l}\right)_f\right\} c_{l_\delta}}{\left[1 + c_{l_\alpha}\left(\frac{\alpha_i}{c_l}\right)_\alpha\right]\left[1 + \left(\frac{\Delta C_{L_{SC}}}{c_l}\right)_\beta\right] - \left(\frac{\alpha_i}{c_l}\right)_\beta\left(\frac{\Delta C_{L_{SC}}}{c_l}\right)_\alpha c_{l_\alpha}} \tag{19}$$

$$\left(\Delta C_{L_\delta}\right)_{SC} = \frac{\left\{\left[1 + \left(\frac{\alpha_i}{c_l}\right)_\alpha c_{l_\alpha}\right]\left(\frac{\Delta C_{L_{SC}}}{c_l}\right)_f - \left(\frac{\alpha_i}{c_l}\right)_f\left(\frac{\Delta C_{L_{SC}}}{c_l}\right)_\alpha c_{l_\alpha}\right\} c_{l_\delta}}{\left[1 + c_{l_\alpha}\left(\frac{\alpha_i}{c_l}\right)_\alpha\right]\left[1 + \left(\frac{\Delta C_{L_{SC}}}{c_l}\right)_\beta\right] - \left(\frac{\alpha_i}{c_l}\right)_\beta\left(\frac{\Delta C_{L_{SC}}}{c_l}\right)_\alpha c_{l_\alpha}} \tag{20}$$

Substituting these values in equation (16) gives

$$C_{L_\delta} = \frac{c_{l_\delta}\left(\left[1+\left(\frac{\Delta C_{L_{SC}}}{c_l}\right)_\beta\right]\left\{1+c_{l_\alpha}\left[\left(\frac{\alpha_i}{c_l}\right)_\alpha-\left(\frac{\alpha_i}{c_l}\right)_f\right]\right\}-\left(\frac{\Delta C_{L_{SC}}}{c_l}\right)_f\left\{1+c_{l_\alpha}\left[\left(\frac{\alpha_i}{c_l}\right)_\alpha-\left(\frac{\alpha_i}{c_l}\right)_\beta\right]\right\}+\left(\frac{\Delta C_{L_{SC}}}{c_l}\right)_\alpha\left[\left(\frac{\alpha_i}{c_l}\right)_f-\left(\frac{\alpha_i}{c_l}\right)_\beta\right]\right)}{\left[1+c_{l_\alpha}\left(\frac{\alpha_i}{c_l}\right)_\alpha\right]\left[1+\left(\frac{\Delta C_{L_{SC}}}{c_l}\right)_\beta\right]-\left(\frac{\alpha_i}{c_l}\right)_\beta\left(\frac{\Delta C_{L_{SC}}}{c_l}\right)_\alpha c_{l_\alpha}} \tag{21}$$

Slope of lift curve C_{L_α}.- If in equation (21) c_{l_α} is substituted for c_{l_δ}, C_{L_α} for C_{L_δ}, and α for subscripts f, the resulting expression gives the slope of the lift against angle-of-attack curve for an elliptic wing; that is

$$C_{L_\alpha} = \frac{c_{l_\alpha}\left\{\left[1+\left(\frac{\Delta C_{L_{SC}}}{c_l}\right)_\beta\right]-\left(\frac{\Delta C_{L_{SC}}}{c_l}\right)_\alpha\right\}}{\left[1+c_{l_\alpha}\left(\frac{\alpha_i}{c_l}\right)_\alpha\right]\left[1+\left(\frac{\Delta C_{L_{SC}}}{c_l}\right)_\beta\right]-\left(\frac{\alpha_i}{c_l}\right)_\beta\left(\frac{\Delta C_{L_{SC}}}{c_l}\right)_\alpha c_{l_\alpha}} \tag{22}$$

Slope of curve of hinge-moment coefficient against flap deflection C_{h_δ}.- The hinge-moment parameter C_{h_δ} of a full-span constant-percentage-chord flap on an elliptic wing may be expressed by an equation similar to equation (16),

$$C_{h_\delta} = c_{h_\delta} - \left(\frac{\alpha_i}{\delta}\right)_{LS} c_{h_\alpha} + \left(\Delta C_{h_\delta}\right)_{SC} \tag{23}$$

Values of $\left(\alpha_i/\delta\right)_{LS}$ are given by equation (19), and $\left(\Delta C_{h_\delta}\right)_{SC}$ is evaluated by a relationship similar to equation (20),

$$\left(\Delta C_{h_\delta}\right)_{SC} = \frac{\left\{\left[1 + \left(\frac{\alpha_i}{c_l}\right)_\alpha c_{l_\alpha}\right]\left(\frac{\Delta C_{h_{SC}}}{c_l}\right)_f - \left(\frac{\alpha_i}{c_l}\right)_f \left(\frac{\Delta C_{h_{SC}}}{c_l}\right)_\alpha c_{l_\alpha}\right\} c_{l_\delta}}{\left[1 + c_{l_\alpha}\left(\frac{\alpha_i}{c_l}\right)_\alpha\right]\left[1 + \left(\frac{\Delta C_{L_{SC}}}{c_l}\right)_\beta\right] - \left(\frac{\alpha_i}{c_l}\right)_\beta \left(\frac{\Delta C_{L_{SC}}}{c_l}\right)_\alpha c_{l_\alpha}} \tag{24}$$

Slope of curve of hinge-moment coefficient against angle of attack C_{h_α}.- The equation for the estimation of C_{h_α} from section data is obtained by substituting α for δ in equation (23), which gives

$$C_{h_\alpha} = c_{h_\alpha} - \left(\frac{\alpha_i}{\alpha}\right)_{LS} c_{h_\alpha} + \left(\Delta C_{h_\alpha}\right)_{SC} \tag{25}$$

By the same procedure equation (24) becomes

$$\left(\Delta C_{h_\alpha}\right)_{SC} = \frac{\left(\frac{\Delta C_{h_{SC}}}{c_l}\right)_\alpha c_{l_\alpha}}{\left[1 + c_{l_\alpha}\left(\frac{\alpha_i}{c_l}\right)_\alpha\right]\left[1 + \left(\frac{\Delta C_{L_{SC}}}{c_l}\right)_\beta\right] - \left(\frac{\alpha_i}{c_l}\right)_\beta \left(\frac{\Delta C_{L_{SC}}}{c_l}\right)_\alpha c_{l_\alpha}} \tag{26}$$

Extension of Formulas to Other Aspect Ratios and Plan Forms

Lift-curve slope C_{L_α}.- The formula for determining the slope of the lift curve from lifting-line theory (reference 14) is

$$C_{L_\alpha} = \frac{f c_{l_\alpha} A}{A + \frac{57.3 c_{l_\alpha}}{\pi}} \tag{27}$$

The values of f presented in reference 14 for wings of different aspect ratios and taper ratios were always between 1.0 and 0.98. Since the value of c_{l_α} will seldom be known to within 2 percent it is probably satisfactory to assume $f = 1.0$.

The slope of the lift curve including the Jones edge-velocity correction is (reference 9), if $c_{l_\alpha} = 0.109$ per degree (2π per radian),

$$C_{L_\alpha} = \frac{0.109A}{AE + 2}$$

If c_{l_α} is not 0.109 the slope of the lift curve with the Jones edge-velocity correction may be shown to be

$$C_{L_\alpha} = \frac{c_{l_\alpha} A}{AE + \frac{57.3 c_{l_\alpha}}{\pi}} \tag{28}$$

In reference 6 the concept of an effective edge-velocity correction E_e was introduced, the value of E_e being selected such that the downwash met the airfoil boundary condition $w = \alpha V$ at the 0.75c point. Numerical values of E_e are given in reference 6. Thus, the final formula for the slope of the lift curve for small angles of attack is

$$C_{L_\alpha} = \frac{A c_{l_\alpha}}{AE_e + \frac{57.3 c_{l_\alpha}}{\pi}} \tag{29}$$

In figure 10 is given a comparison of the values of C_{L_α} calculated by this formula and by other theoretical methods for a value of $c_{l_\alpha} = 0.109$ per degree or 2π per radian.

Effectiveness parameter $(\alpha_\delta)_{C_L}$.- According to the assumptions of lifting-line theory, the parameter $(\alpha_\delta)_{c_l}$ is independent of aspect-ratio effects. From lifting-line theory, the lift due to the deflection of an elevator C_{L_δ} may be found, thus

$$C_{L_{\delta_{LL}}} = \int_{-1}^{1} (\alpha_\delta)_{c_l} \frac{d\left(\frac{C_L}{\Delta\alpha}\right)}{d\left(\frac{y}{b/2}\right)} d\left(\frac{y}{b/2}\right) \tag{30a}$$

or

$$C_{L_{\delta_{LL}}} = \int_{-1}^{1} \left(\alpha_\delta\right)_{c_l} \, d\left(\frac{C_L}{\Delta\alpha}\right) \tag{30b}$$

where curves of $C_L/\Delta\alpha$ against $\frac{y}{b/2}$ may be obtained from the calculation of the lift caused by the deflection of ailerons of various spans such as those used in reference 15. Because

$$\left(\alpha_\delta\right)_{C_{L_{LL}}} = \left|\frac{C_{L_{\delta_{LL}}}}{C_{L_{\alpha_{LL}}}}\right|$$

and

$$C_{L_{\alpha_{LL}}} = 2\left(\frac{C_L}{\Delta\alpha}\right)_{max}$$

equation (1) is obtained

$$\left(\alpha_\delta\right)_{C_{L_{LL}}} = \int_{0}^{1.0} \left(\alpha_\delta\right)_{c_l} \, d\left[\frac{C_L/\Delta\alpha}{\left(C_L/\Delta\alpha\right)_{max}}\right]$$

Numerical values of $\frac{C_L/\Delta\alpha}{\left(C_L/\Delta\alpha\right)_{max}}$ were calculated for the wings of reference 15 and are presented in figure 2. Because there is a greater lifting-surface-theory correction to $C_{L_{\alpha_{LL}}}$ than to $C_{L_{\delta_{LL}}}$, there is a lifting-surface-theory correction to $\left(\alpha_\delta\right)_{C_{L_{LL}}}$. The corrected

value of $\left(\alpha_\delta\right)_{C_L}$ for full-span elevators may be estimated by computing C_{L_δ} similarly to C_{L_α} from equation (11); that is,

$$C_{L_\delta} = \frac{Ac_{l_\alpha}\left(\alpha_\delta\right)_{c_l}}{AE_{e_f} + \frac{57.3c_{l_\alpha}}{\pi}}$$

where E_{e_f} is an effective edge-velocity correction determined for flap-type chordwise loadings. Thus,

$$\left(\alpha_\delta\right)_{C_L} = \left|\frac{C_{L_\delta}}{C_{L_\alpha}}\right| = \frac{\dfrac{Ac_{l_\alpha}\left(\alpha_\delta\right)_{c_l}}{AE_{e_f} + \dfrac{57.3c_{l_\alpha}}{\pi}}}{\dfrac{Ac_{l_\alpha}}{AE_e + \dfrac{57.3c_{l_\alpha}}{\pi}}} \tag{31}$$

and

$$\frac{\left(\alpha_\delta\right)_{C_L}}{\left(\alpha_\delta\right)_{c_l}} = \frac{E_e + \dfrac{57.3c_{l_\alpha}}{\pi A}}{E_{e_f} + \dfrac{57.3c_{l_\alpha}}{\pi}} \tag{32}$$

The values of the effective edge-velocity correction E_{e_f} used in the determination of C_{L_δ} and $\left(\alpha_\delta\right)_{C_L}/\left(\alpha_\delta\right)_{c_l}$ were determined in the following manner:

Values of C_{L_δ} were computed from equation (21) for a series of flap-chord ratios and an aspect ratio 3. Values of E_{e_f} were then determined so that, for a section slope of the lift curve of 2π, C_{L_δ} given by equation (21) was equal to

$$C_{L_\delta} = \frac{2\pi A\left(\alpha_\delta\right)_{c_l}}{AE_{e_f} + 2}$$

The values of E_{e_f} obtained in this manner for various flap-chord ratios were then extended to other aspect ratios by use of the relationship

$$E_{e_f} = K\left(E_e - 1\right) + 1$$

as previously suggested. The values of E_{e_f} determined for elliptic wings in this manner are assumed to apply to wings of other plan forms.

Hinge-moment angle-of-attack slope C_{h_α}.- The finite-span value of the slope of the curve of hinge-moment coefficient plotted against angle of attack as given by lifting-line theory is

$$C_{h_{\alpha_{LL}}} = \frac{1}{\frac{b_e}{b}\,\bar{c}_e^{\,2}} \int_0^{b_e/b} c_{h_\alpha}\left(\frac{\alpha - \alpha_{i_{LL}}}{\alpha}\right) c_e^{\,2}\, d\left(\frac{y}{b/2}\right) \tag{33}$$

where $\alpha_{i_{LL}}$ is the lifting-line theory value of the induced angle of attack at each section $\frac{y}{b/2}$. Reference 6 shows that the complete value of the induced

angle of attack is given by the lifting-surface-theory value of the downwash angle at the 0.5c points and that this value for a wing at an angle of attack is larger than that given by lifting-line theory. A further lifting-surface-theory correction resulting from the effective-camber changes must also be applied. In the past the induced angle of attack has been estimated by use of the Jones edge-velocity correction, and the streamline-curvature correction for hinge-moment coefficients has been used uncorrected for aerodynamic induction (references 1 and 6). The effect of aerodynamic induction is to reduce the streamline-curvature load by a small increment of angle-of-attack-type load. The final value of streamline curvature is not altered but the final value of angle of attack is. The method developed in the section "General Lifting-Surface-Theory Formula for the Determination of Aerodynamic Characteristic of Elliptic Wings from Section Data" takes into account the change in induced angle of attack caused by the streamline curvature.

For tail surfaces of approximately elliptic plan form, α_i may be considered constant across the span. For either rectangular or highly tapered tail surfaces, $\alpha_{i_{LL}}$ varies markedly across the span. Lifting-surface-theory results for the downwash at the 0.5c points are not available for wings other than elliptical; however, a satisfactory approximation to the induced angle of attack may be obtained by calculating the variation in the induced angle along the span from lifting-line theory for the particular plan form and estimating the additional lifting-surface-theory induced angle for an equivalent elliptic wing of the same aspect ratio. The variation in the induced angle across the span is calculated as the ratio of the induced angle at each section to the induced angle for the equivalent elliptic wing, both calculated by means of lifting-line theory. These calculations were made by the method presented in reference 16. Two types of plan form were considered: straight taper with square tips and straight taper with elliptic tips covering 15 percent of the span. The results are presented in figure 9. Thus,

$$C_{h_\alpha} = \frac{1}{\frac{b_e}{b}\,\bar{c}_e^{\,2}} \int_0^{b_e/b} c_{h_\alpha} \left[1 - \left(\frac{\alpha_i}{\alpha}\right)_{LS(ell)} \left(\frac{\alpha_i}{\alpha_{i_{ell}}}\right)_{LL}\right] c_e^{\,2} \; d\left(\frac{y}{b/2}\right)$$

$$+ \left(\Delta C_{h_\alpha}\right)_{SC} \tag{34}$$

For tail surfaces of nearly elliptic plan form (λ between 0.4 and 0.6) and having elevators of nearly constant-percentage chord so that c_{h_α} is almost constant, equation (34) may be simplified to equation (3)

$$C_{h_\alpha} = \left(c_{h_\alpha}\right)_{av_\alpha} \left[1 - \left(\frac{\alpha_{i_{ell}}}{\alpha}\right)_{LS}\right] + \left(\Delta C_{h_\alpha}\right)_{SC}$$

When $\left(c_{h_\alpha}\right)_{av_\alpha}$ cannot be averaged by eye, it may be evaluated from

$$\left(c_{h_\alpha}\right)_{av_\alpha} = \frac{1}{\frac{b_e}{b}\,\bar{c}_e^{\,2}} \int_0^{b_e/b} c_{h_\alpha} \left\{\frac{\left[1 - \left(\frac{\alpha_i}{\alpha}\right)_{LS} \left(\frac{\alpha_i}{\alpha_{i_{ell}}}\right)_{LL}\right]}{\left[1 - \left(\frac{\alpha_{i_{ell}}}{\alpha}\right)_{LS}\right]}\right\} c_e^{\,2} \; d\left(\frac{y}{b/2}\right)$$

which is equivalent to equation (4). The curves of $\left(\frac{\alpha_e}{\alpha_{e_{ell}}}\right)_{LS}$, which is equal to $\dfrac{1 - \left(\frac{\alpha_i}{\alpha}\right)_{LS} \left(\frac{\alpha_i}{\alpha_{i_{ell}}}\right)_{LL}}{1 - \left(\frac{\alpha_{i_{ell}}}{\alpha}\right)_{LS}}$, were

computed by use of values of $\left(\alpha_i/\alpha\right)_{LS}$ for elliptic wings from figure 4 and values of $\left(\alpha_i/\alpha_{i_{ell}}\right)_{LL}$ from figure 9.

Values of $\left(\Delta C_{h_\alpha}\right)_{SC}$ may be estimated from the parameter $\left(\Delta C_{h_\delta}\right)_{SC} \frac{\left(c_e/c\right)^2}{F\eta c_{l_\delta}} A\left(A\sqrt{1 - M^2} + 4.21\right)\sqrt{1 - M^2}$ for elliptic wings presented in figure 5. (Use curve labeled $\frac{c_e}{c} = 1.0$ and substitute c_{l_α} for c_{l_δ}.) Methods for determining the factor $\frac{F}{\left(c_e/c\right)^2}$ for externally balanced elevators are discussed in references 6 and 10 and values are presented in figure 7(a). Values of the factor were calculated for internally balanced elevators and are given in figure 7(b). Values of the aspect-ratio factor $\frac{1}{A\left(A\sqrt{1 - M^2} + 4.21\right)\sqrt{1 - M^2}}$ are shown in figure 6. The value of η is $1 - 0.0005\phi^2$.

Hinge-moment-elevator-deflection slope C_{h_δ}.- From lifting-line theory,

$$C_{h_\delta} = \frac{1}{\frac{b_e}{b}\bar{c}_e^2}\left[\int_0^{b_e/b} c_{h_\delta} c_e^2 \, d\left(\frac{y}{b/2}\right) - \int_0^{b_e/b} c_{h_\alpha}\left(\frac{\alpha_i}{\delta}\right)_{LL} c_e^2 \, d\left(\frac{y}{b/2}\right)\right] \tag{35}$$

As for the C_{h_α} calculation, lifting-surface-theory values of $\left(\alpha_i/\delta\right)_{LS}$ and the camber correction $\left(\Delta C_{h_\delta}\right)_{SC}$ must be estimated from the values computed for elliptic wings (equations (19) and (24)).

The evaluation of $\alpha_{i_{LS}}$ for C_{h_δ} is similar to its evaluation for C_{h_α}. Values of $\left(\alpha_i/\delta\right)_{LS}$ for elliptic wings may be obtained from figure 4 by use of an average value of c_e/c over the span of the elevator. It is then assumed that this value may be corrected to the proper plan form by multiplying by the ratio of the induced angle along the span from lifting-line theory for the particular plan form to the induced angle for the elliptic wing from lifting-line theory. Values of this ratio $\left(\alpha_i/\alpha_{i_{ell}}\right)_{LL}$ are presented in figure 9 for various plan forms.

It is assumed that the streamline-curvature correction $\left(\Delta C_{h_\delta}\right)_{SC}$ may be evaluated from figures 5, 6, and 7 by use of an average value of c_e/c,

$$C_{h_\delta} = \frac{1}{\frac{b_e}{b}\,\bar{c}_e^{\,2}}\left[\int_0^{b_e/b} c_{h_\delta} c_e^{\,2}\, d\left(\frac{y}{b/2}\right) - \left(\frac{\alpha_i}{\delta}\right)_{LS}\int_0^{b_e/b}\left(\frac{\alpha_i}{\alpha_{i_{ell}}}\right)_{LL} c_{h_\alpha} c_e^{\,2}\, d\left(\frac{y}{b/2}\right)\right] + \left(\Delta C_{h_\delta}\right)_{SC}$$

which is equivalent to equation (5).

Elevator-hinge-moment-tab-deflection slope $C_{h_{\delta_t}}$.- The aspect-ratio corrections to $C_{h_{\delta_t}}$ (the slope of the curve of elevator hinge moment plotted against tab deflection) are from about one-half to one-fourth of the aspect-ratio correction to c_{h_δ}. In fact, in reference 7 an empirical correlation of the parameter $C_{h_{\delta_t}}$ was made that was based solely on geometric characteristics (strip theory). Because the correlation was satisfactory

the aspect-ratio corrections, especially for partial-span tabs, may be assumed small enough to allow the variation of these corrections with total-surface configuration to be neglected. Thus, a constant reduction factor of about 0.9 may be used with satisfactory accuracy. For completeness, however, the lifting-surface-theory values of the aspect-ratio corrections will be presented for the case of full-span tabs along with an estimate of the approximate magnitude of the corrections. For partial-span tabs the load induced by the tabs on the part of the elevator to either side of the tab appears to neutralize a large part of the small decrease in load which occurs over the elevator and tab. The aspect-ratio corrections for the full-span tab arrangement are thus the larger.

From lifting-line theory, for an elliptic wing

$$C_{h_{\delta_t}} = c_{h_{\delta_t}} - \left(\frac{\alpha_i}{\alpha}\right)_{LL} \left(\alpha_{\delta_t}\right)_{c_l} c_{h_\alpha} \tag{36}$$

and from lifting-surface theory, for an elliptic wing

$$C_{h_{\delta_t}} = c_{h_{\delta_t}} - \left(\frac{\alpha_i}{\alpha}\right)_{LS} \left(\alpha_{\delta_t}\right)_{c_l} c_{h_\alpha} + \left(\Delta C_{h_{\delta_t}}\right)_{SC} \tag{37}$$

To a first approximation, $\left(\Delta C_h/C_L\right)_{SC}$ may be assumed to be the same for any flap- or tab-chord ratio, thus,

$$\left(\Delta C_{h_{\delta_t}}\right)_{SC} \approx \left(\Delta C_{h_\delta}\right)_{SC} \left(\frac{\delta}{\delta_t}\right)_{c_l} \approx \left(\Delta C_{h_\delta}\right)_{SC} \frac{\left(\alpha_{\delta_t}\right)_{c_l}}{\left(\alpha_\delta\right)_{c_l}} \tag{38}$$

where

$$C_{h_{\delta_t}} = c_{h_{\delta_t}} - \frac{\left(\alpha_{\delta_t}\right)_{c_l}}{\left(\alpha_\delta\right)_{c_l}} \left[\left(\frac{\alpha_i}{\alpha}\right)_{LS} \left(\alpha_\delta\right)_{c_l} c_{h_\alpha} - \left(\Delta C_{h_\delta}\right)_{SC}\right] \tag{39}$$

The expression in the brackets in equation (39) is equal to the reduction in c_{h_δ} caused by plan form (equation (5)). The reduction in $c_{h_{\delta_t}}$ is therefore equal to the reduction in c_{h_δ} times the ratio $\frac{(a_{\delta_t})_{c_l}}{(a_\delta)_{c_l}}$. In order to estimate the magnitude of the aspect-ratio correction $c_{h_\delta} \approx c_{h_{\delta_t}}$ and $\frac{(a_{\delta_t})_{c_l}}{(a_\delta)_{c_l}} \approx \frac{1}{2.5}$ may be used for usual tab-elevator-chord ratios of about 0.2. (See reference 17.) Also from reference 1, $C_{h_\delta} \approx 0.5c_{h_\delta}$; therefore, the reduction in $c_{h_{\delta_t}}$ caused by aerodynamic induction is approximately 0.4 of the reduction in c_{h_δ} and, further, $C_{h_{\delta_t}} \approx 0.8c_{h_{\delta_t}}$ for a full-span tab.

Equation (39) may usually be used to estimate $C_{h_{\delta_t}}$ for full-span-tab arrangements with sufficient accuracy.

EXPERIMENTAL VERIFICATION

Results of wind-tunnel tests are available for three finite-span models of horizontal tails of NACA 0009 section and aspect ratio 3 (references 4 and 5 and unpublished data). These tail surfaces have rectangular, elliptical, and linearly tapered 2:1 plan forms. All have full-span elevators.

In each of these reports, tables are presented giving a comparison of the experimental values and the values computed for C_{L_α} by use of the Jones edge-velocity correction, and for C_{h_α} by use of both the Jones

edge-velocity correction and the additional aspect-ratio correction resulting from the aerodynamically induced elliptic loading (reference 1). At the time of publication of reference 1 no values of the correction for C_{h_δ} were available.

For the various arrangements for which data are available, values of C_{L_α}, $(\alpha_\delta)_{C_L}$, C_{h_α}, and C_{h_δ} were computed by the method presented herein and are presented in table I.

The agreement between the measured and the calculated values for all the parameters is believed to be satisfactory considering the probable accuracy of the measured data, although the estimated values of the parameter $(\alpha_\delta)_{C_L}$ seem slightly greater than those obtained by lifting-line theory and the aspect-ratio corrections to C_{h_δ} for the elevators without overhang balance do not seem to be quite large enough. The three-dimensional boundary-layer flows, especially for the tapered wing model with a sweptforward and beveled trailing edge, is believed to be the main cause of the discrepancy. The aspect-ratio corrections for the elevators with overhang balance, however, are slightly too large. The lifting-surface-theory aspect-ratio corrections are generally much more accurate than the lifting-line-theory corrections; however, the values of C_{h_δ} computed by means of lifting-line theory are in fair agreement for the elevators with moderate amounts of overhang balance.

CONCLUDING REMARK

The lifting-surface-theory method presented is believed to allow a satisfactory estimation of the lift and hinge-moment parameters of horizontal-tail surfaces with full-span elevators from the section data. The application of the method is fairly simple and requires no knowledge of lifting-surface theory. A comparison

of experimental finite-span lift and hinge-moment parameters for three horizontal tail surfaces with the parameters estimated by the method provided a satisfactory verification of the method.

Langley Memorial Aeronautical Laboratory
National Advisory Committee for Aeronautics
Langley Field, Va., April 25, 1946

REFERENCES

1. Swanson, Robert S., and Gillis, Clarence L.: Limitations of Lifting-Line Theory for Estimation of Aileron Hinge-Moment Characteristics. NACA CB No. 3L02, 1943.

2. Swanson, Robert S., and Crandall, Stewart M.: An Electromagnetic-Analogy Method of Solving Lifting-Surface-Theory Problems. NACA ARR No. L5D23, 1945.

3. Crandall, Stewart M.: Lifting-Surface-Theory Results for Thin Elliptic Wings of Aspect Ratio 3 with Chordwise Loadings Corresponding to 0.5-Chord Plain Flap and to Parabolic-Arc Camber. NACA TN No. 1064, 1946.

4. Tamburello, Vito, Smith, Bernard J., and Silvers, H. Norman: Wind-Tunnel Investigation of Control-Surface Characteristics of Plain and Balanced Flaps on an NACA 0009 Elliptical Semispan Wing. NACA ARR No. L5L18, 1946.

5. Garner, I. Elizabeth: Wind-Tunnel Investigation of Control-Surface Characteristics. XX - Plain and Balanced Flaps on an NACA 0009 Rectangular Semispan Tail Surface. NACA ARR No. L4I11f, 1944.

6. Swanson, Robert S., and Priddy, E. LaVerne: Lifting-Surface-Theory Values of the Damping in Roll and of the Parameter Used in Estimating Aileron Stick Forces. NACA ARR No. L5F23, 1945.

7. Crandall, Stewart M., and Murray, Harry E.: Analysis of Available Data on the Effects of Tabs on Control-Surface Hinge Moments. NACA TN No. 1049, 1946.

8. Krienes, Klaus: The Elliptic Wing Based on the Potential Theory. NACA TM No. 971, 1941.

9. Jones, Robert T.: Theoretical Correction for the Lift of Elliptic Wings. Jour. Aero. Sci., vol. 9, no. 1, Nov. 1941, pp. 8-10.

10. Swanson, Robert S., and Toll, Thomas A.: Jet-Boundary Corrections for Reflection-Plane Models in Rectangular Wind Tunnels. NACA ARR No. 3E22, 1943.

11. Falkner, V. M.: The Calculation of Aerodynamic Loading on Surfaces of Any Shape. R. & M. No. 1910, British A.R.C., 1943.

12. Cohen, Doris: A Method for Determining the Camber and Twist of a Surface to Support a Given Distribution of Lift. NACA TN No. 855, 1942.

13. Goldstein, S., and Young, A. D.: The Linear Perturbation Theory of Compressible Flow with Applications to Wind-Tunnel Interference. R. & M. No. 1909, British A.R.C., 1943.

14. Anderson, Raymond F.: Determination of the Characteristics of Tapered Wings. NACA Rep. No. 572, 1936.

15. Pearson, Henry A., and Jones, Robert T.: Theoretical Stability and Control Characteristics of Wings with Various Amounts of Taper and Twist. NACA Rep. No. 635, 1938.

16. Hildebrand, Francis B.: A Least-Squares Procedure for the Solution of the Lifting-Line Integral Equation. NACA TN No. 925, 1944.

17. Sears, Richard I.: Wind-Tunnel Data on the Aerodynamic Characteristics of Airplane Control Surfaces. NACA ACR No. 3L08, 1943.

TABLE I

COMPUTATION OF FINITE-SPAN WING CHARACTERISTICS FROM SECTION DATA

[NACA 0009 airfoil; aspect ratio of 3]

Model characteristics						Section aerodynamic characteristics used in estimating finite-span characteristics				Finite-span aerodynamic characteristics											
										C_{L_α}			$(\alpha_0)_{C_L}$			C_{h_α}			C_{h_δ}		
λ	β (deg)	c_e/c	c_b/c	Gap	Balance nose shape	c_{l_α}	$(\alpha_0)_{c_l}$	c_{h_α}	c_{h_δ}	Lifting-line theory	Lifting-surface theory	Measured value	Lifting-line theory	Lifting-surface theory	Measured value	Lifting-line theory	Lifting-surface theory	Measured value	Lifting-line theory	Lifting-surface theory	Measured value
Elliptic	11.6	0.50	----	Sealed	Plain	0.100	0.78	-0.0104	-0.0140	0.062	0.053	0.052	0.78	0.80	0.75	-0.0065	-0.0044	-0.0036	-0.0109	-0.0097	-0.0080
Elliptic	11.6	.50	----	0.005c	Plain	.096	.76	-.0104	-.0140	.060	.052	.050	.76	.78	.74	-.0066	-.0045	-.0042	-.0111	-.0090	-.0078
0.50	11.1	.30	----	Sealed	Plain	.100	.59	-.0058	-.0119	.062	.053	.054	.59	.62	.65	-.0036	-.0020	-.0021	-.0106	-.0092	-.0092
.50	11.1	.30	----	.005c	Plain	.096	.60	-.0063	-.0117	.060	.052	.053	.60	.63	.57	-.0038	-.0023	-.0030	-.0103	-.0091	-.0089
.50	11.1	.30	0.35	Sealed	Elliptic	.096	.60	-.0030	-.0073	.060	.052	.053	.60	.63	.66	-.0019	-.0007	-.0015	-.0066	-.0055	-.0060
.50	11.1	.30	.35	.005c	Elliptic	.090	.55	-.0029	-.0062	.058	.050	.052	.55	.58	.55	-.0019	-.0007	-.0013	-.0056	-.0046	-.0053
.50	19.8	.30	----	Sealed	Plain	.095	.57	-.0022	-.0085	.060	.052	.053	.57	.60	.58	-.0014	-.0001	-.0002	-.0080	-.0068	-.0069
.50	19.8	.30	----	.005c	Plain	.090	.54	-.0018	-.0066	.058	.050	.051	.54	.57	.53	-.0012	0	-.0003	-.0059	-.0052	-.0053
.50	29.6	.30	----	Sealed	Plain	.091	.55	.0019	-.0046	.059	.050	.050	.55	.58	.50	.0012	.0020	.0024	-.0050	-.0042	-.0016
.50	29.6	.30	----	.005c	Plain	.086	.46	.0031	-.0008	.056	.048	.048	.46	.48	.46	.0020	.0026	.0034	-.0014	-.0007	-.0001
1.00	11.6	.30	----	Sealed	Plain	.100	.59	-.0058	-.0119	.062	.053	.055	.59	.62	.64	-.0036	-.0020	-.0020	-.0106	-.0092	-.0082
1.00	11.6	.30	----	.005c	Plain	.096	.60	-.0063	-.0117	.060	.052	.054	.60	.63	.60	-.0038	-.0023	-.0024	-.0103	-.0091	-.0080
1.00	11.6	.30	0.35	Sealed	Blunt	.096	.64	-.0028	-.0058	.060	.052	.054	.64	.67	.64	-.0018	-.0006	-.0005	-.0031	-.0019	-.0028
1.00	11.6	.30	.35	.005c	Blunt	.090	.68	-.0017	-.0037	.056	.050	.050	.68	.70	.67	-.0011	0	.0009	-.0035	-.0022	-.0025
1.00	11.6	.30	.35	Sealed	Elliptic	.096	.60	-.0030	-.0073	.060	.052	.055	.60	.63	.62	-.0019	-.0007	-.0010	-.0066	-.0055	-.0060
1.00	11.6	.30	.35	.005c	Elliptic	.090	.55	-.0029	-.0062	.058	.050	.050	.55	.58	.58	-.0019	-.0007	0	-.0056	-.0046	-.0052

NATIONAL ADVISORY
COMMITTEE FOR AERONAUTICS

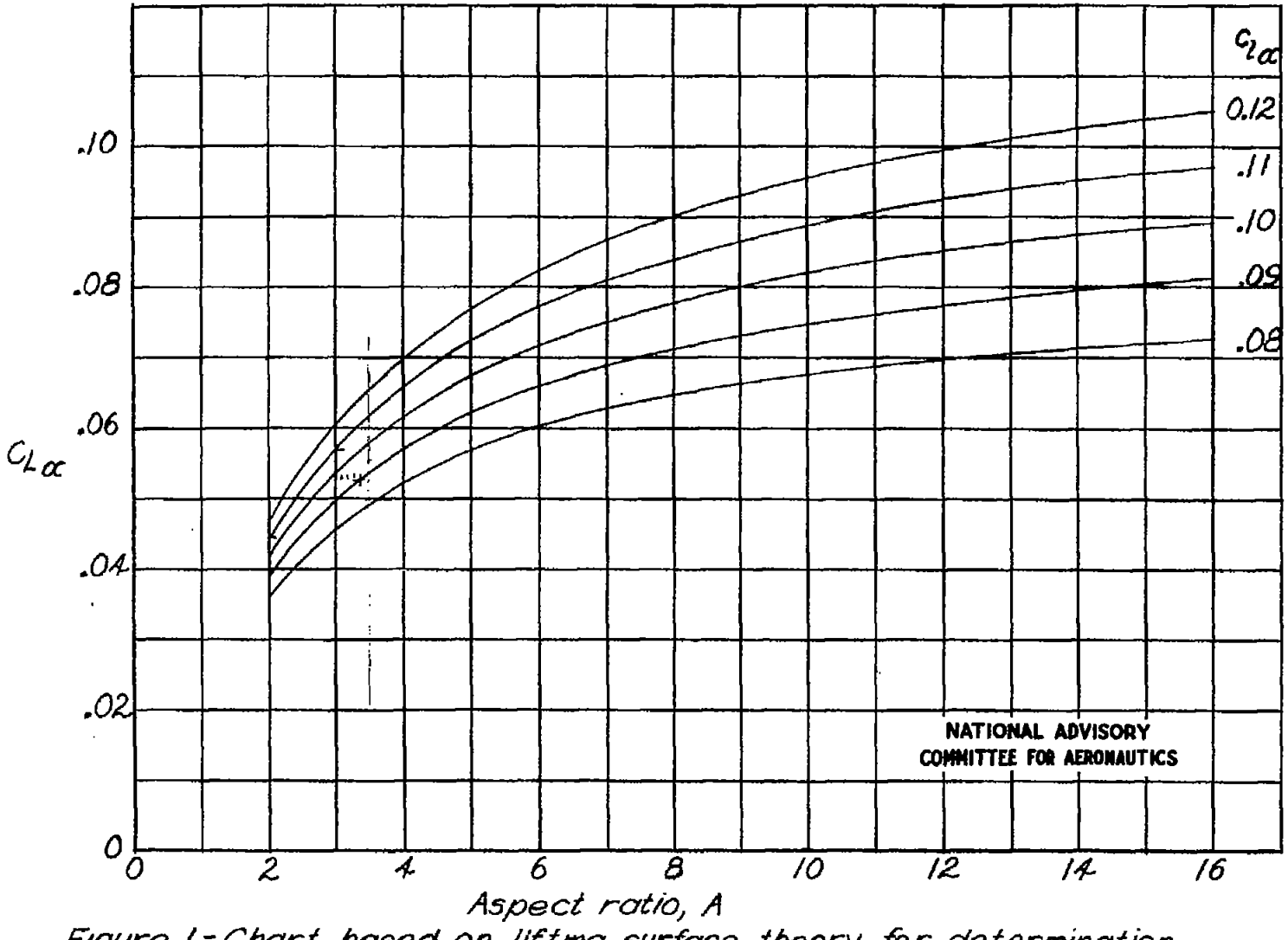

Figure 1.- Chart based on lifting-surface theory for determination of the slope of the lift curve for small angles of attack.

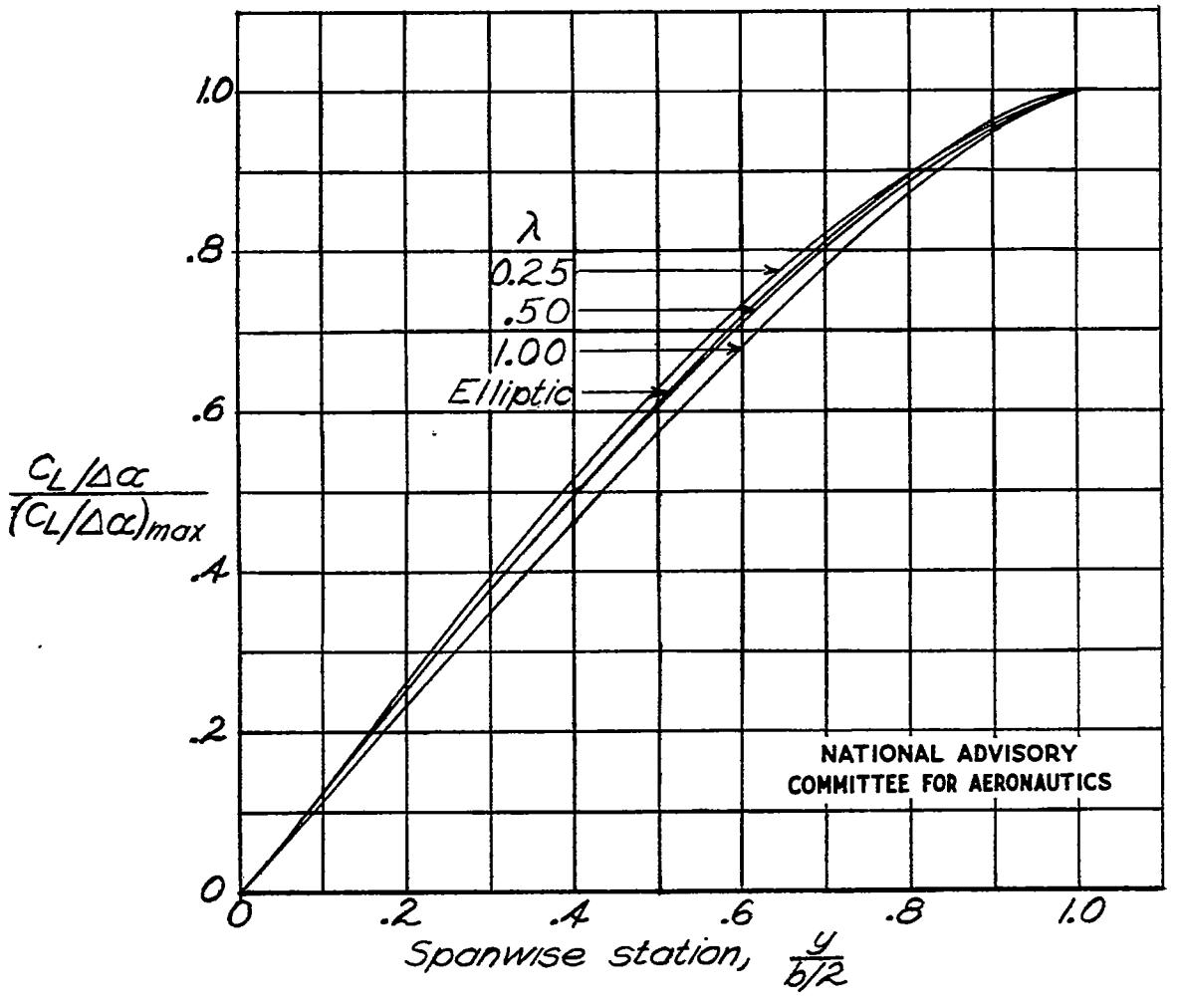

Figure 2.- Chart based on lifting-line theory for the determination of the effective value of section effectiveness parameter $(\alpha_\delta)_{c_l}$ for horizontal tails with elevators having chords not a constant percentage of the wing chord.

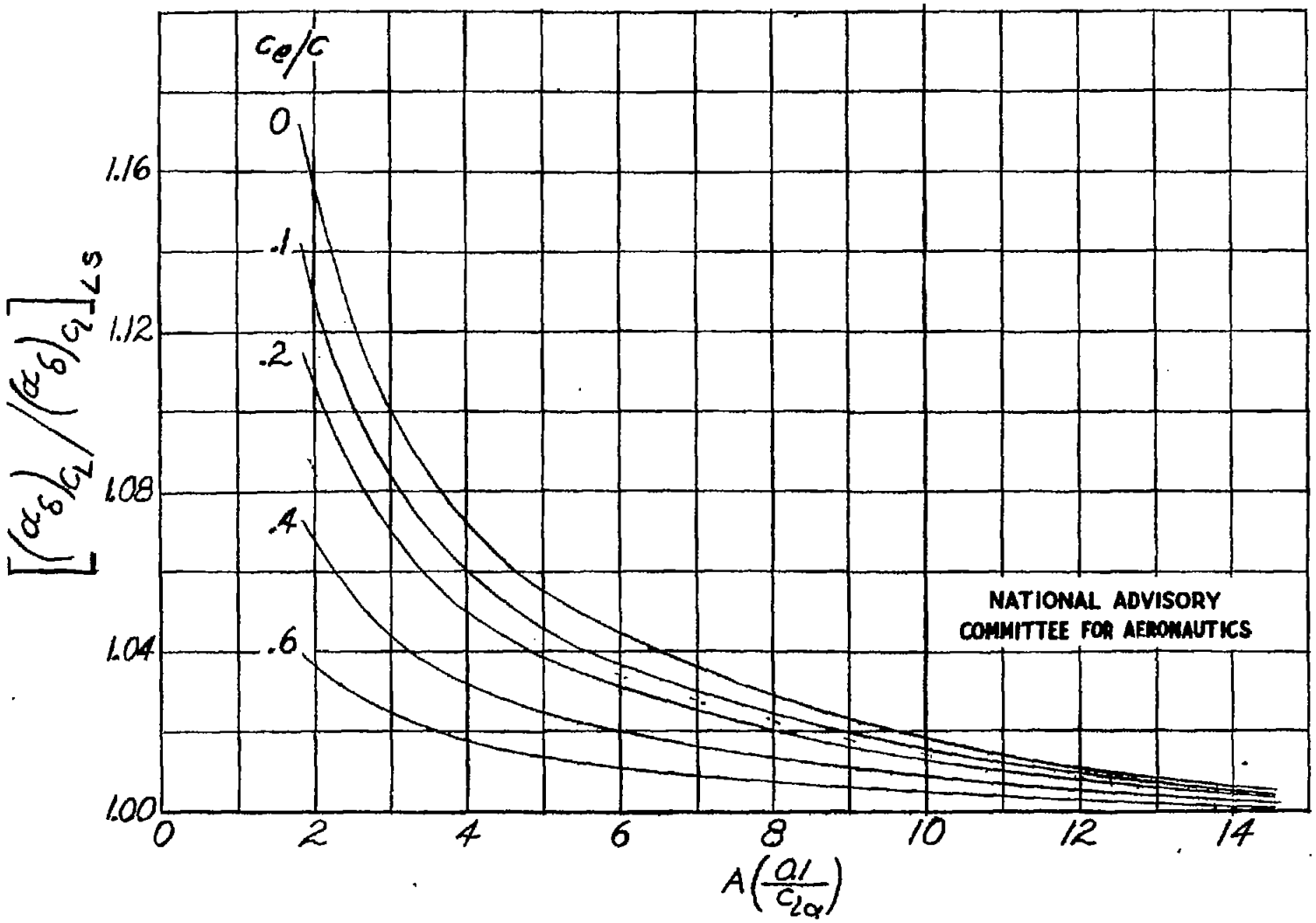

Figure 3.- Chart based on lifting-surface theory for the evaluation of the finite-span lift effectiveness parameter, $(\alpha_\delta)_{c_L}$.

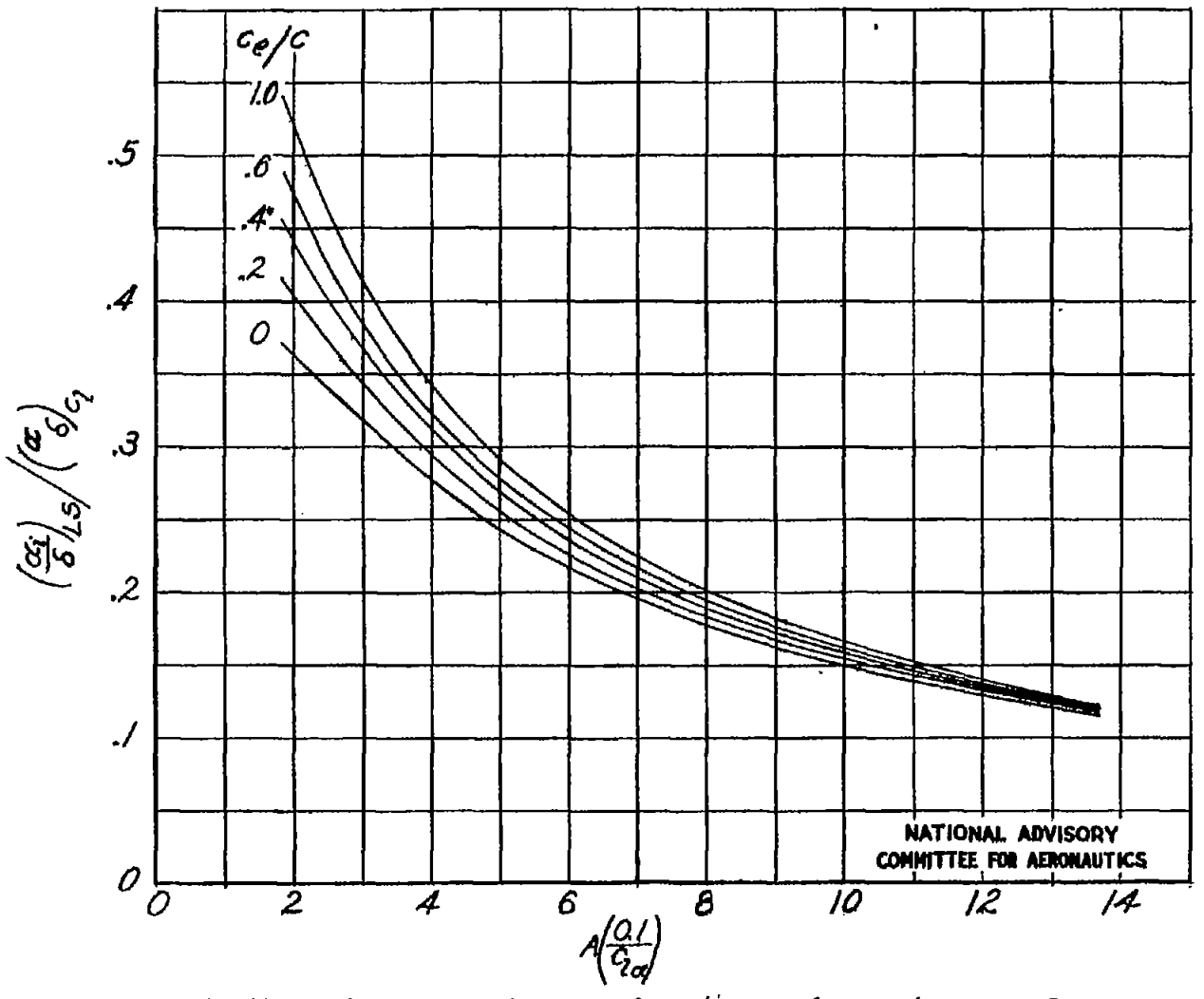

Figure 4.- Chart based on lifting-surface theory for evaluation of induced angle of attack for unit geometric angle of attack or elevator deflection.

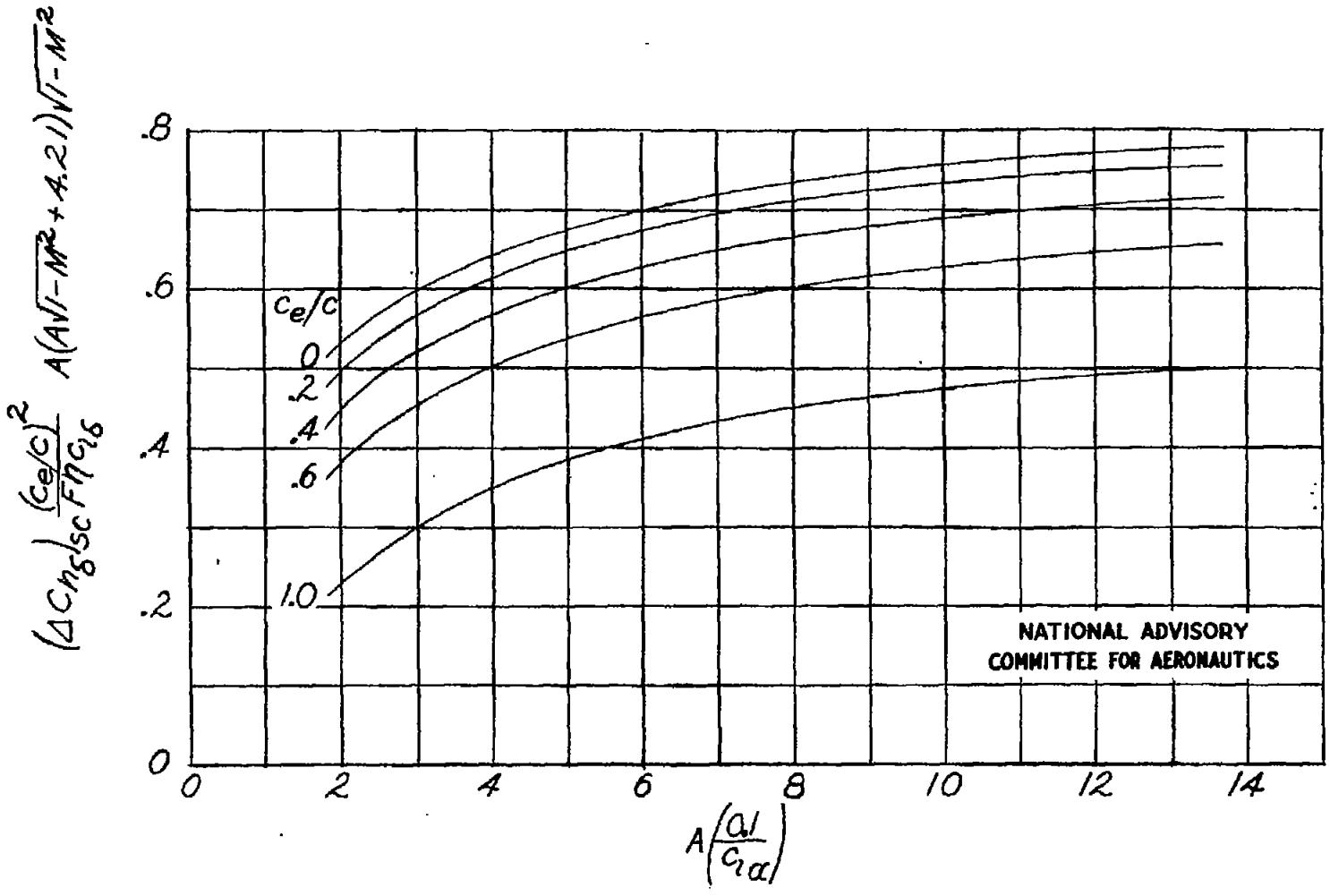

Figure 5.- Chart based on lifting-surface theory for the determination of the increment of hinge-moment coefficient caused by induced elliptic chordwise loading.

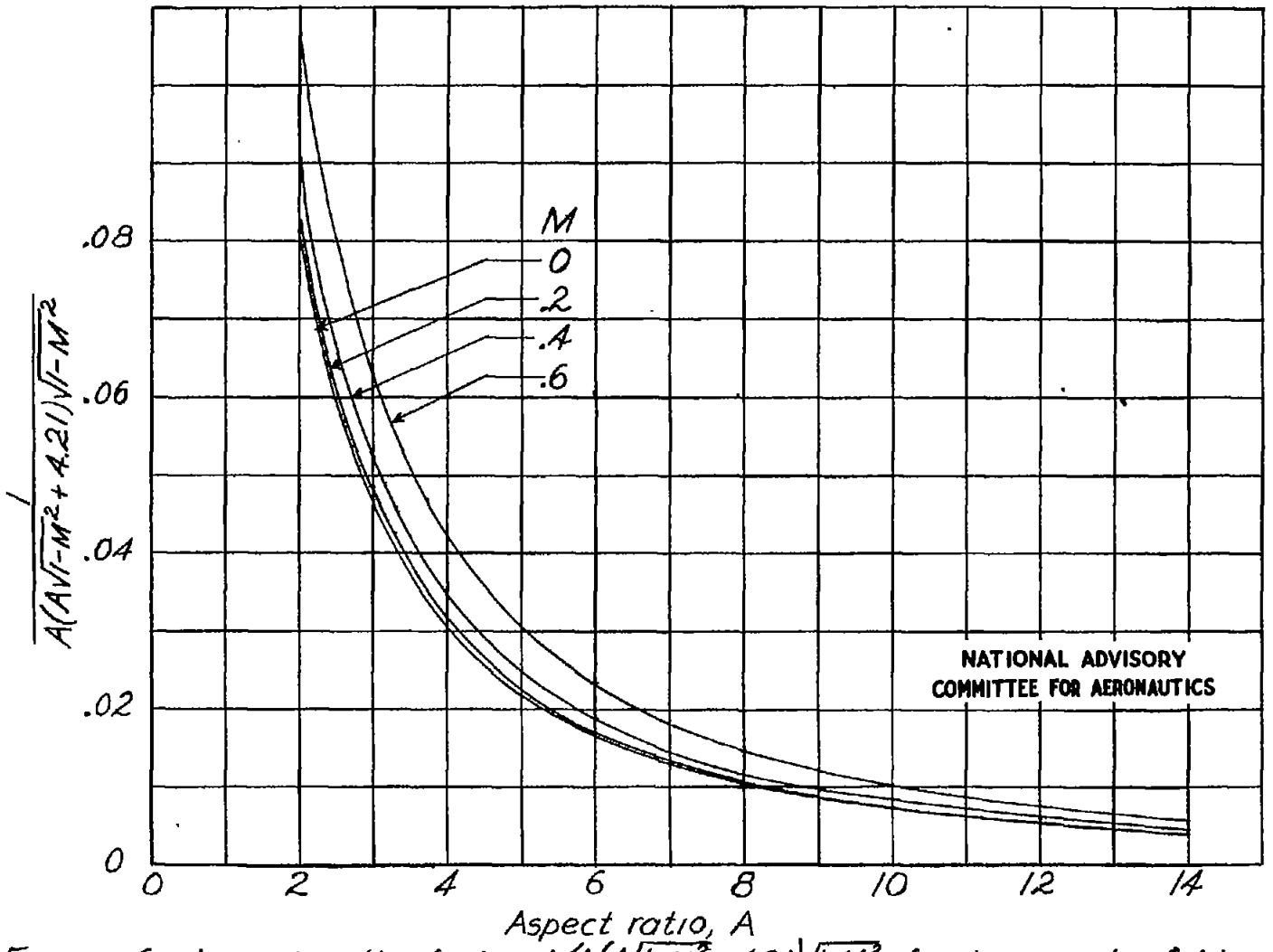

Figure 6.- Aspect ratio factor $1/A(A\sqrt{1-M^2}+4.21)\sqrt{1-M^2}$ for increment of hinge-moment caused by induced elliptic chordwise load.

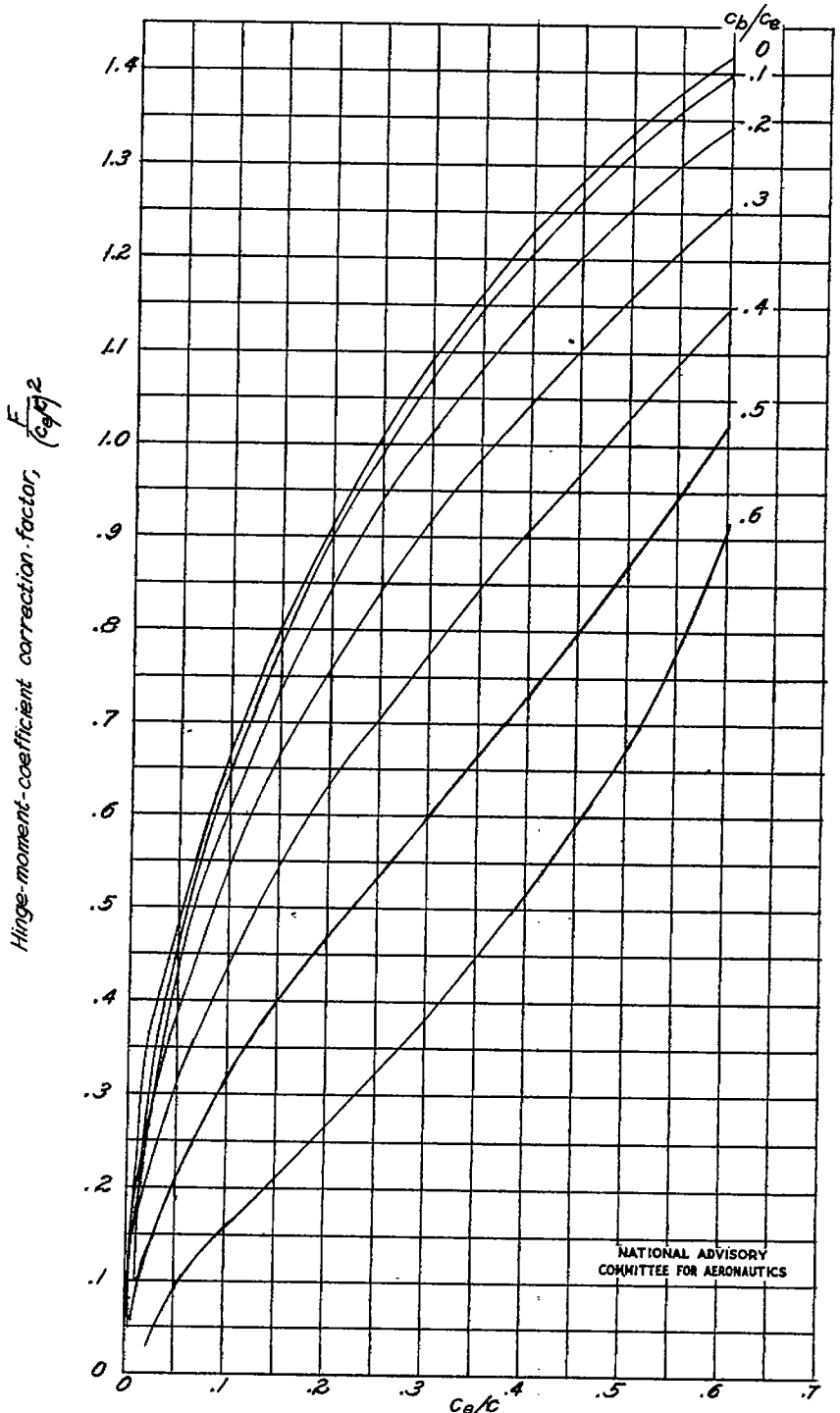

(a) Plain nose and external-overhang aerodynamic balances.

Figure 7.- Chart based on thin airfoil theory for evaluation of the hinge-moment correction factor $F/(c_e/c)^2$ for elevators.

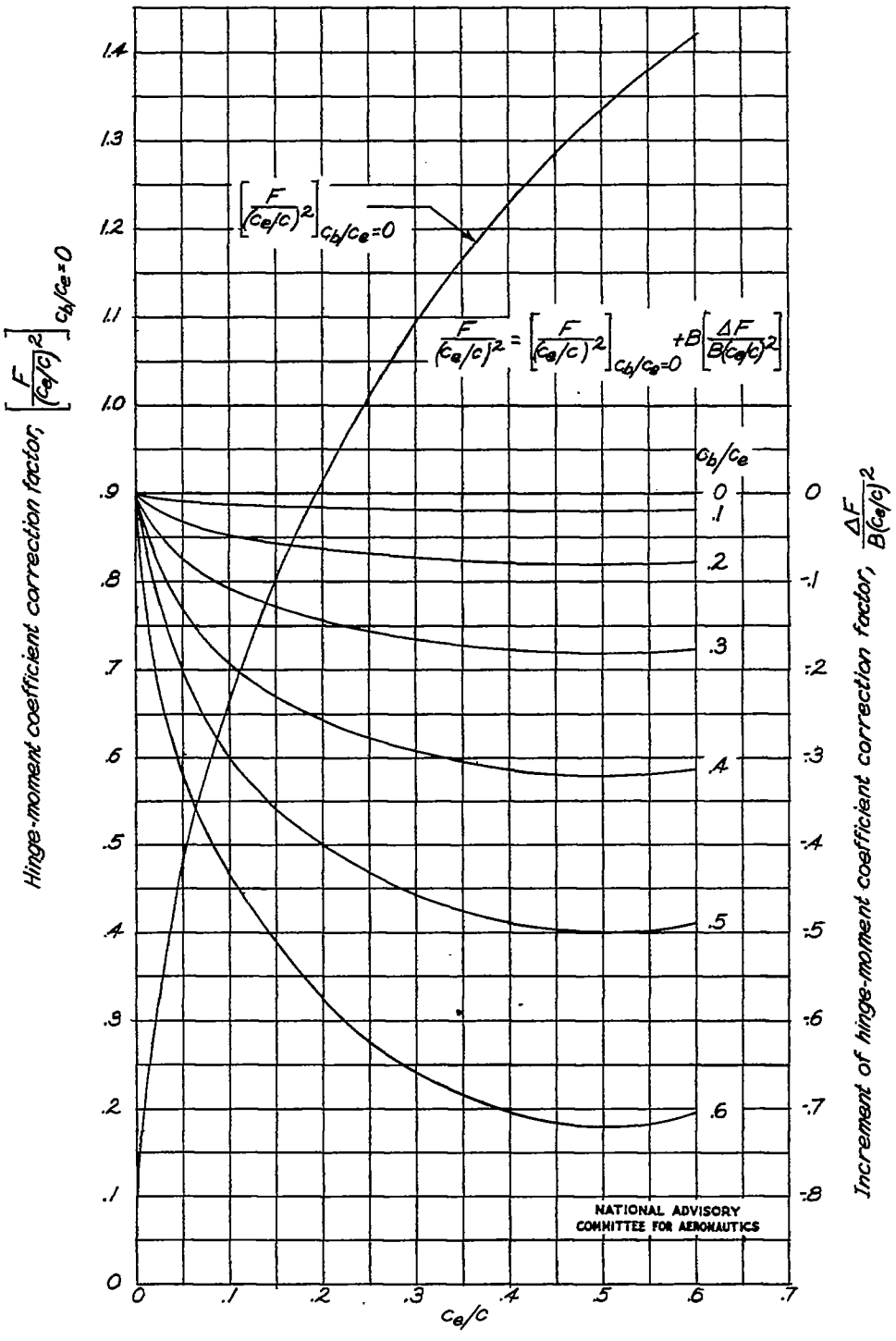

(b) Internal aerodynamic balances.

Figure 7.- Concluded.

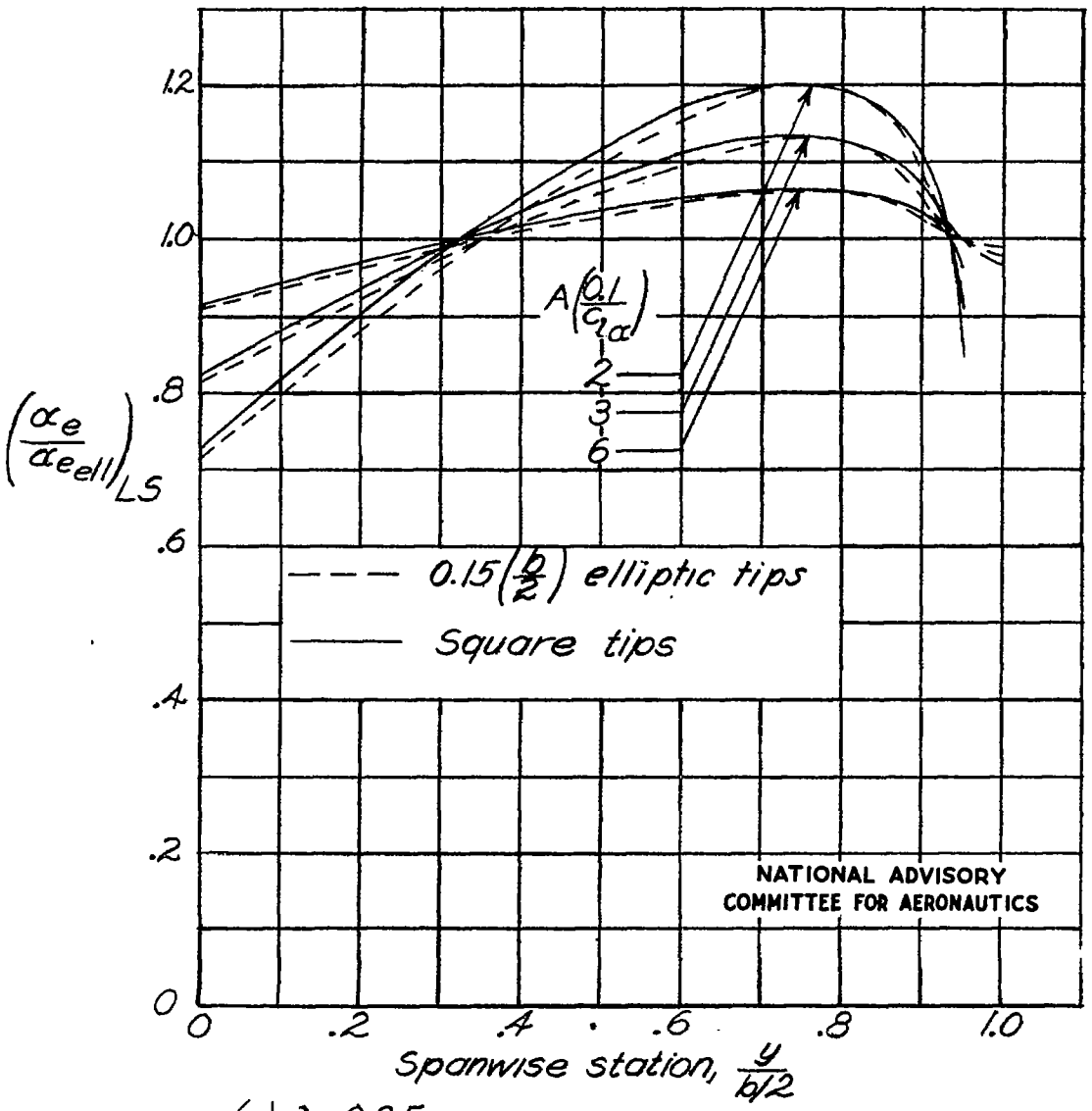

(a) $\lambda = 0.25$.

Figure 8.- Chart for the determination of the parameter $(\alpha_e/\alpha_{e_{ell}})_{LS}$.

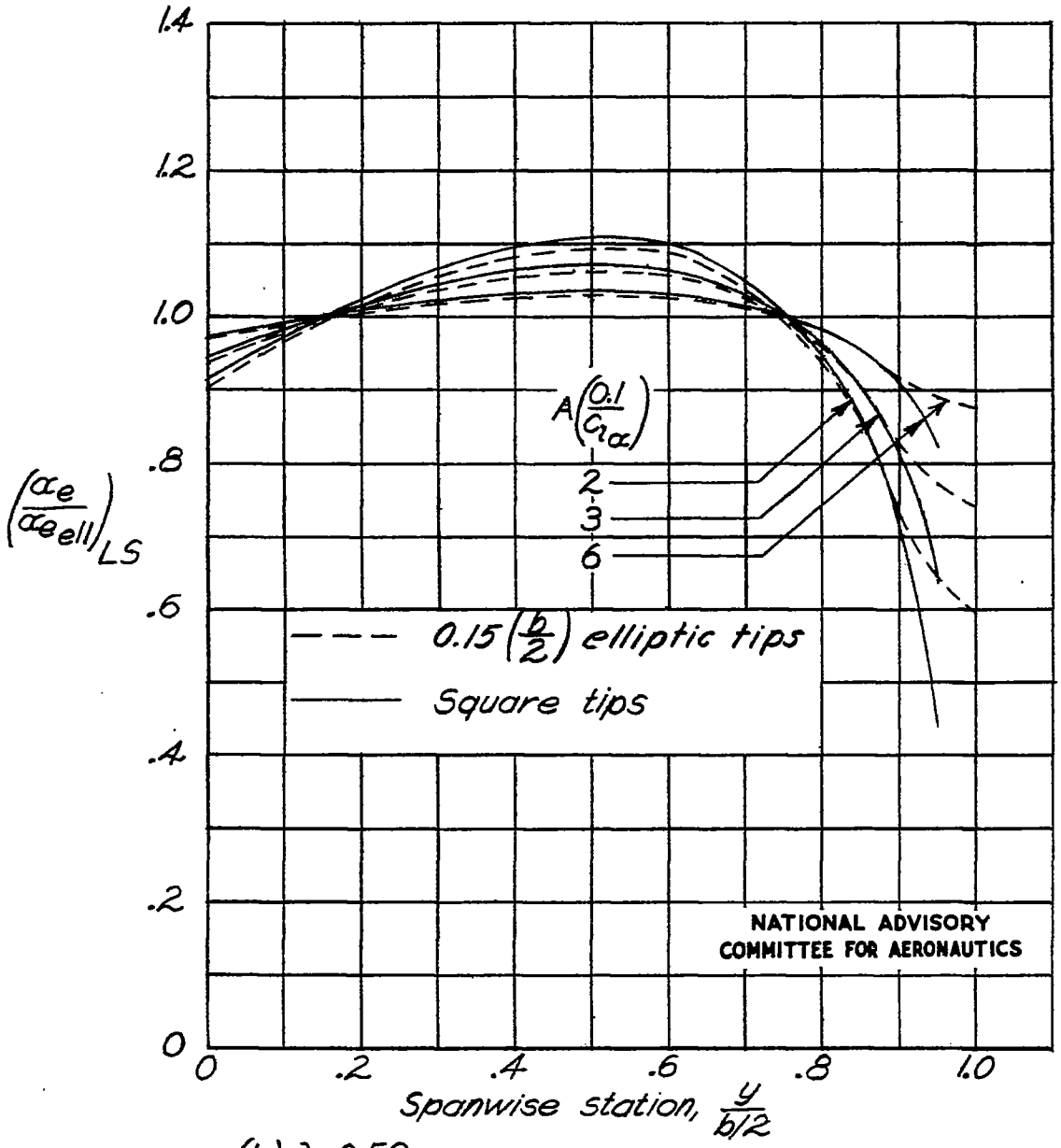

(b) $\lambda = 0.50$.

Figure 8.- Continued.

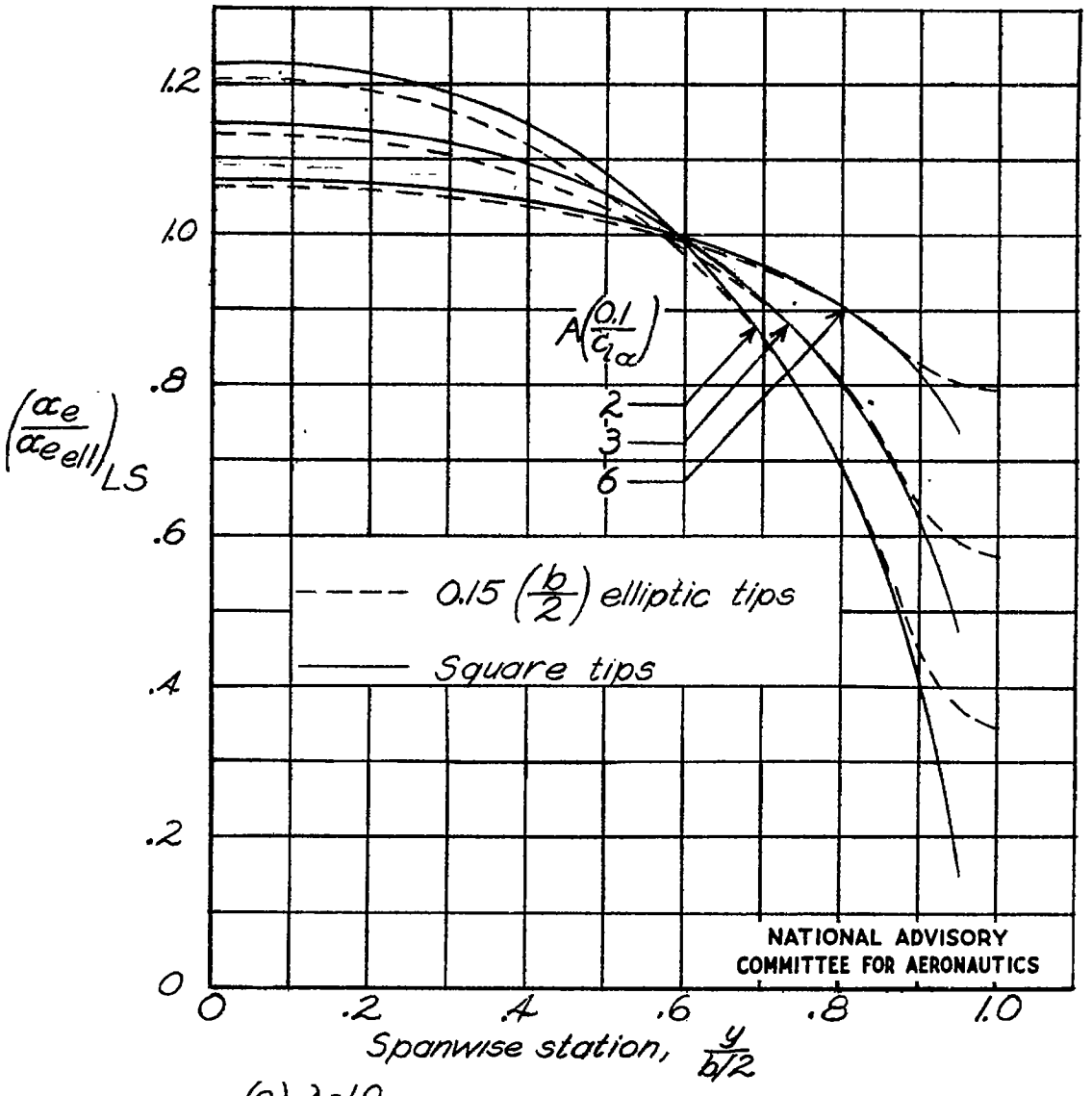

(c) $\lambda = 1.0$.

Figure 8.- Concluded.

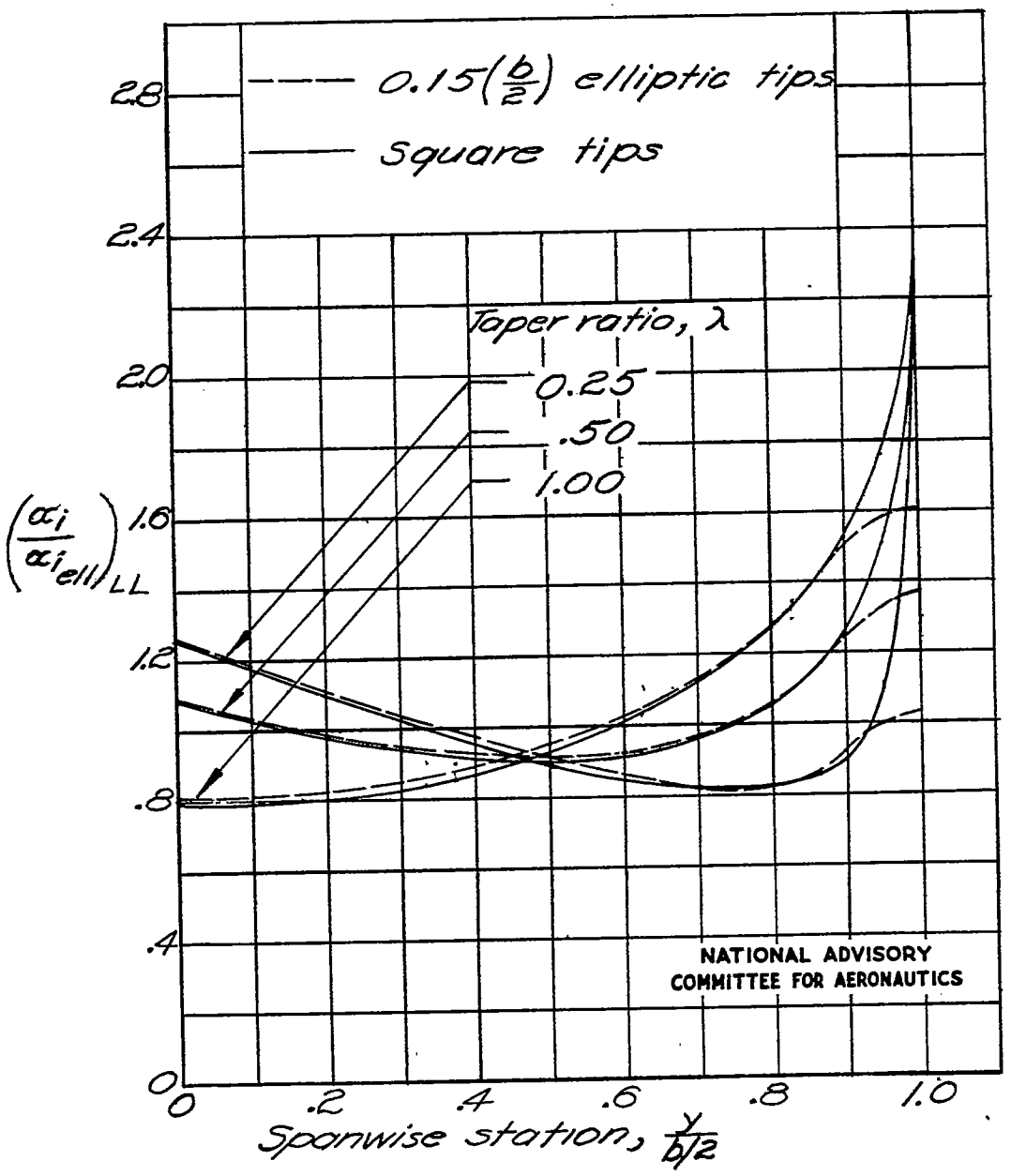

Figure 9.- Chart based on lifting-line theory for determination of the parameter $(\alpha_i/\alpha_{i_{ell}})_{LL}$.

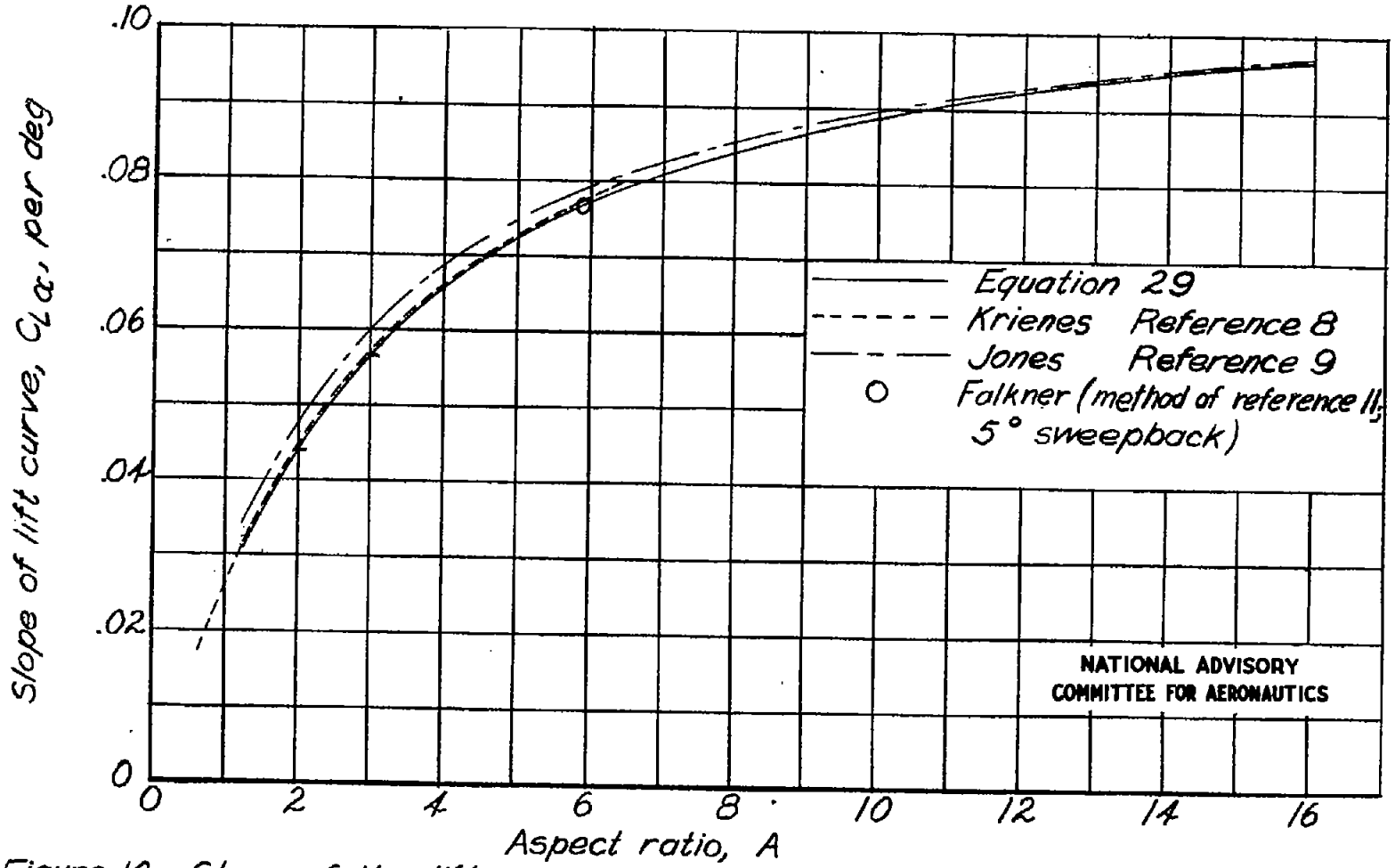

Figure 10.- Slope of the lift curve, C_{L_α}, as calculated by various theoretical methods for a section slope of 2π/radian, $M = 0$.

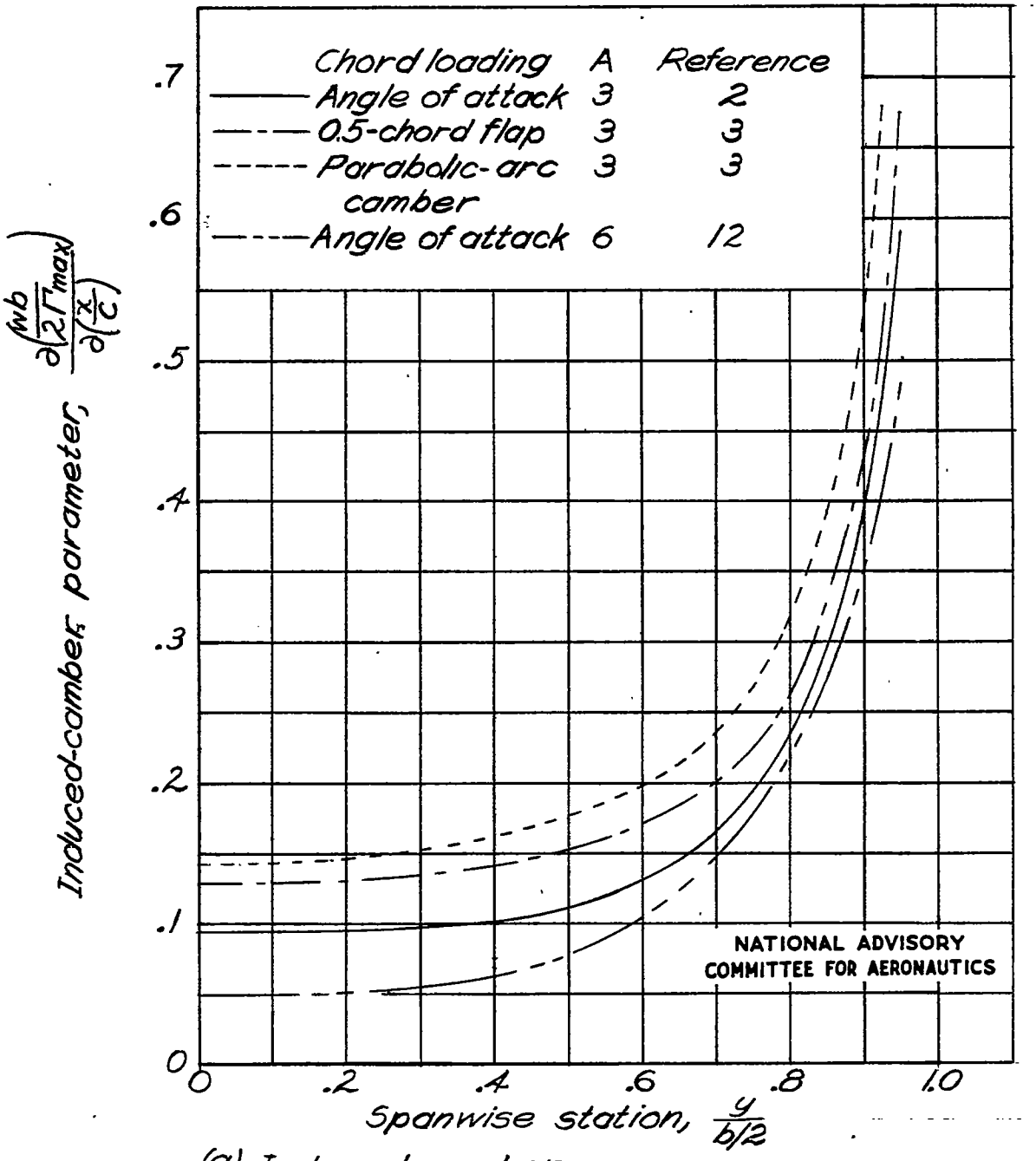

(a) Induced camber.

Figure 11.- Summary of available lifting-surface-theory solutions.

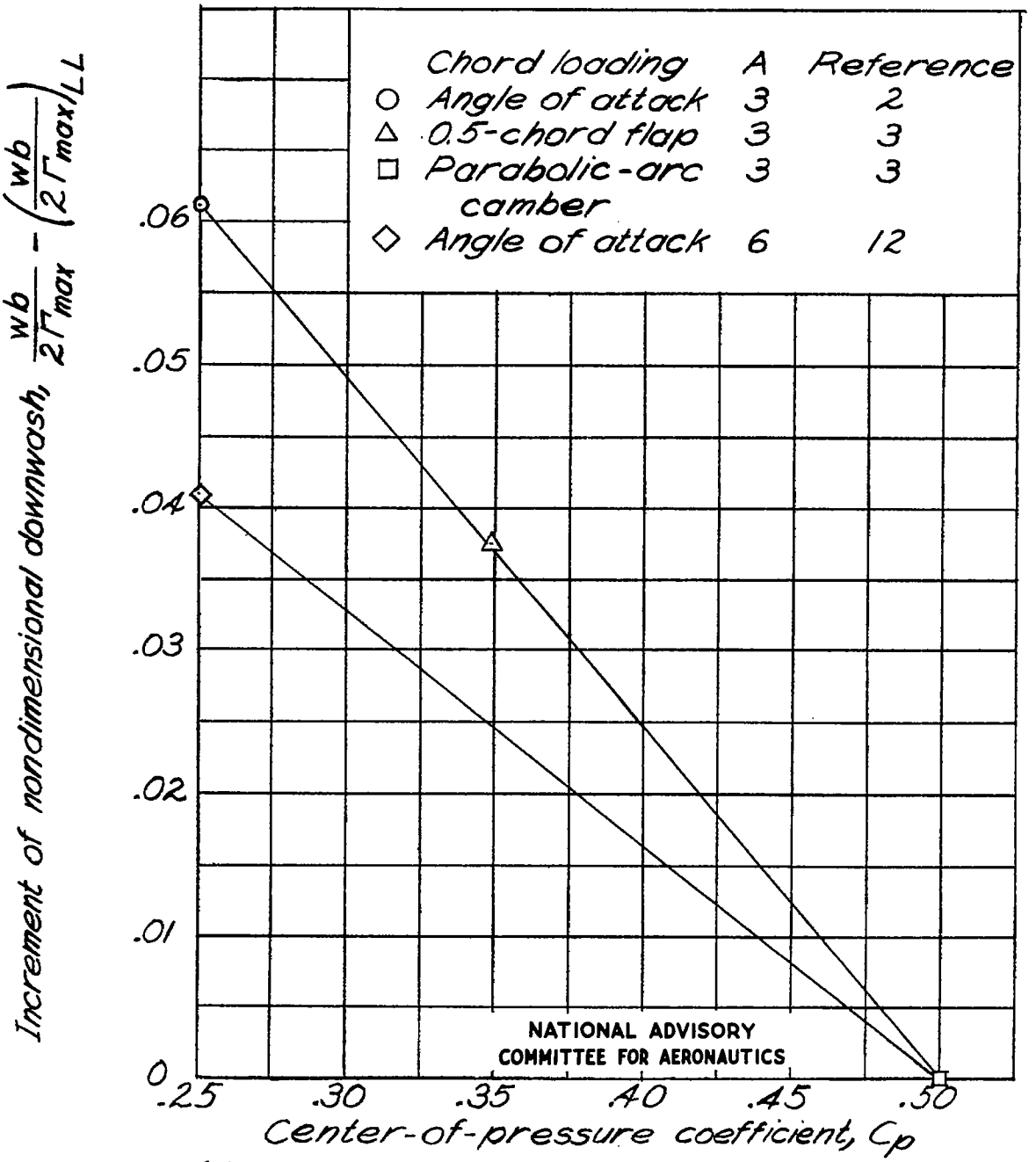

(b) Induced downwash at the 0.5-chord line.

Figure 11.- Concluded.

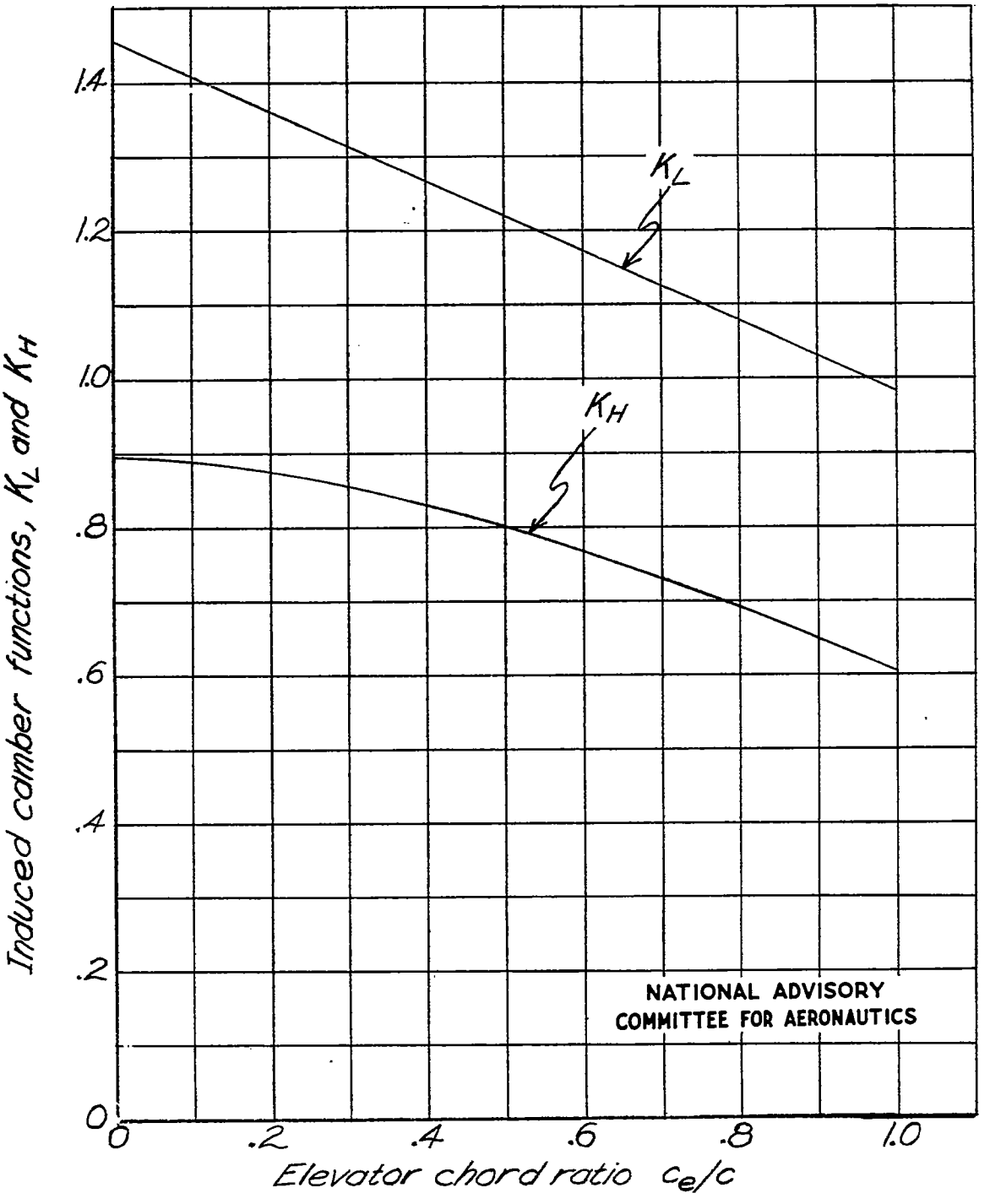

Figure 12.- Variation of the induced camber functions K_L and K_H with elevator-chord ratio.